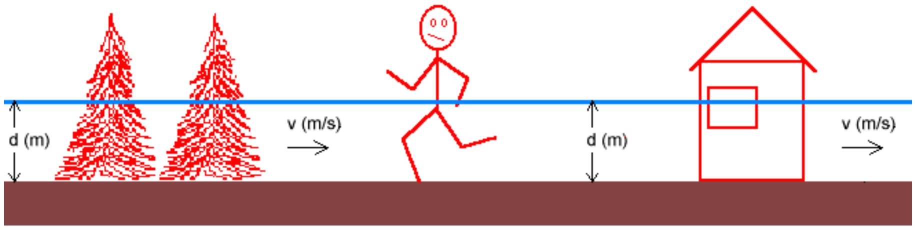

RESCDAM

Final report of Helsinki University of Technology
THE USE OF PHYSICAL MODELS
IN DAM-BREAK FLOOD ANALYSIS

11 December 2000

The use of physical models in dam-break flood analysis

I. flow resistance of tree stand

II. flow resistance of group of buildings

III. human stability in flowing water

CONTENTS

FIGURES

TABLES

1. INTRODUCTION

The EU-project RESCDAM – Development of rescue actions based on dam-break flood analysis – was launched in 1999 and coordinated by the Finnish Environment Institute. One part of the RESCDAM project was a research carried out at the Laboratory of water resources at the Helsinki University of Technology. The 3 goals of this project was to test 1) human stability and manoeuvrability in flowing water, 2) permanence of houses in flowing water and 3) roughness coefficients of forest and houses. Human stability and manoeuvrability and the permanence of houses in flowing water were studied to produce information for the rescue authorities estimating the risks of a dam break flood and planning the rescue actions. The roughness coefficients of forest and houses were of interest to produce parameters for the mathematical models used to calculate the propagation of dam-break flood.

Human stability and roughness coefficient of forest and houses were studied using physical laboratory tests. Experiments on the human stability were conducted testing full scale test persons in the 130 m long model basin equipped with towing carriage in the Helsinki University of Technology Ship Laboratory. The roughness coefficient was studied in the 50 m long fixed bed flume at the Laboratory of Water Resources using scale model forests and houses. The permanence of houses in flowing water was based on literature.

The laboratory and literature studies were performed by the RESCDAM-group of the Laboratory of water resources at Helsinki University of Technology: professor Tuomo Karvonen, laboratory manager Antti Hepojoki, M.Sc. (Tech.) Jyrki Kotola and a student Hanna-Kaisa Huhta who wrote her master's thesis on this subject and graduated during the project. In addition, a great deal of the test arrangements and practical aspects of the experiments were performed by technicist Antti Louhio. This report was authored by the above mentioned RESCDAM-group.

2. PERMANENCE OF BUILDINGS IN FLOWING WATER

2.1 INTRODUCTION

"The house in a water media is subjected to three major forces: buoyancy, hydrostatic pressure and dynamic pressure." (Black 1975)

Terms (Water Words Dictionary 2000)

- "**Buoyancy** — The tendency of a body to float or rise when submerged in a fluid."
- "**Hydrodynamic Force** — The force exerted by moving water. Contrast with *Hydrostatic Forc*e."
- "**Hydrodynamic Loads** — Forces imposed on structures by floodwaters due other impacts of moving water on the upstream side of the structure, drag along its sides, and eddies or negative pressures on its downstream side."
- "**Hydrostatic Force** — The force exerted by water at rest, including lateral pressure on walls and uplift (buoyancy) on floors. Contrast with *Hydrodynamic Forc*e."
- "**Hydrostatic Loads** — (1) Forces imposed on a flooded structure due to the weight of the water. (2) (Floods) Those loads or pressures resulting from the static mass of water at any point of floodwater contact with a structure. They are equal in all directions and always act perpendicular to the surface on which they are applied. Hydrostatic loads can act vertically on structural members such as floors, decks, and roofs, and can act laterally on upright structural members such as walls, piers, and foundations."
- "**Hydrostatic Pressure** — The pressure in a fluid in equilibrium which is due solely to the weight of fluid above."

"The effects of structural failure on flood damage to the residential and commercial sector have been little discussed in the literature." (Smith 1994)

"For flood proofing purposes, a velocity of 10 fps (3,05 m/s) should be considered the upper limit for which flood proofing measures are effective and economically feasible." (Lardieri 1975).

2.2 CASE STUDY AND DAMAGE CRITERION DEVELOPED BY SANGREY ET AL. (1975)

In the case of a dam-break flood, flood flows are diverted by structures on the flood plain. Diverted flood waters have a potential for doing heavy damage (Sangrey et al. 1975). Sangrey et al. developed a procedure for predicting the interaction of flood waters and structures on the flood plain. They studied the flooding in Chemung river flood plain (Elmira, NY, USA) during the tropical storm Agnes in 1972.

Over 1000 structures of various types were located within the Chemung River flood plain. 155 of these structures were selected for the damage survey. Structures were classified in nine categories to provide an approximate weight (*W*) for each structure (Table 1). The damage survey was done in two parts: 1) detailed examination of aerial photos, 2) ground survey including physical examination and discussion with owners and other residents. The structures were classified either "survived" or "destroyed".

Table 1 Classification of structures (Sangrey et al. 1975)

Symbol	Description	Weight (kg)
A	1 story, light construction frame house	7800
B	1 story, heavy construction frame house	11100
C	1½ story, light construction frame house	11100
D	1½ story, heavy construction frame house	16300
E	2 story, light construction frame house	12600
F	2 story, heavy construction frame house	18800
G	1 story sheds and garages	1000
H	Special heavy structures, commercial masonry, houses more than 2 stories, etc.	Estimated individually
V	Brick veneer frame structures, 1 or 1½ stories	Estimated individually

The prediction of forces exerted by flood waters on structures required that the velocity v (m/s) and depth of the flood waters d (m) at the structure were known. These characteristics of flood flow were predicted by 1D hydrodynamic model (HEC-2). The model was modified by including the effects of the structures on roughness and cross-sectional area. The effects of structures on the flooding area were taken into account by subtracting the structurally blocked area from the total cross-sectional area determined by the bottom topography.

Flood waters produce both a horizontal and a vertical loading on a flood plain structure. The horizontal force is a drag force acting in the downstream direction. It was calculated by assuming a drag coefficient C_D value two and by neglecting the force exerted on the foundation. Sangrey et al. calculated the horizontal load F_H applied to the structure with Equation 1.

$$F_H = C_D \cdot 0{,}5 \cdot \rho \cdot v^2 \cdot b \cdot \left(d\text{-}h_{fo}\right)$$

Equation 1

where C_D = drag coefficient = 2
ρ = water density kg/m^3
v = velocity m/s
b = projected width perpendicular to flow m
d = depth of water m
h_{fo} = foundation height m

Sangrey et al. (1975) did not directly study the effect of foundation type because they think that the most common failure mode of interest is the separation of the structure from its foundation. Sangrey et al. (1975) assumed that when light structural connections (screws and nails) are used across the potential failure surface (foundation) no significant resistance is offered. This assumption is less valid when the foundation bolts, tie down cables and similar flood proofing devices are used (Sangrey et al. 1975).

A nondimensional characteristic parameter F_H/W and a corresponding normal force or buoyancy parameter $(d\text{-}h_{fo})/(10s)$, where s = number of structural stories, on each of the structures were calculated.

The data of the case study is presented in Figure 1. There is a clear and general separation between the destroyed (full symbol) and survived structures (open symbol). Sangrey et al. developed the damage criterion using parameters F_H/W and $(d\text{-}h_{fo})/(10s)$. This empirical damage criterion is presented in Figure 1. For example, if the buoyancy parameter is 0,8 and parameter $F_H/W = 1$ the structure is very likely to be destroyed during the flood.

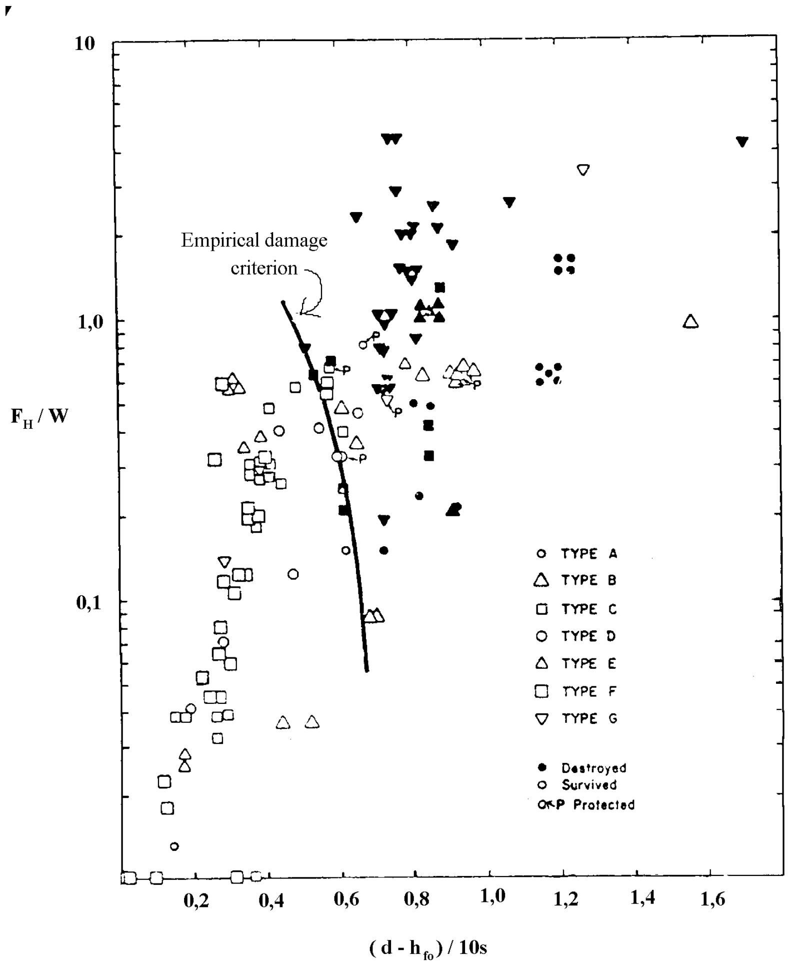

Figure 1 Results of the flood damage survey and empirical damage criterion (Sangrey et al. 1975).

2.3 EVALUATING THE BUOYANCY FORCE (BLACK 1975)

Black analysed three modest frame house types (1 story, 1½ story and 2 story houses) in order to examine the buoyant forces. The houses were conventional unanchored platform frame dwellings, size 7,3 m × 9,8 m. Each house type included two subtypes: I) lighter version with drywall construction and normal wood, II) heavier version with plaster wall construction and heavy wood (plywood). In addition, the effect of a brick veneer on the lower story of the 1½ story house was studied. Weight of the houses without a brick veneer varied from 7100 kg to 17000 kg.

Black calculated the buoyant force as a function of the depth of submergence. House begins to float when the buoyant force equals the weight of the house. Table 2 shows the depth of submergence at which the house begins to float. The light weight frame houses float when the depth of submergence is at about the midpoint of the height of the house. Heavier frame houses float at about the three quarter point of the height.

Table 2 Depth of submergence needed to float a house (Black 1975)

	1 story	1½ story	2 story
version I (lighter, drywall construction)	1,9 m	2,7 m	2,9 m
version II (heavier, plaster wall construction)	2,8 m	3,5 m	4,7 m
version I with brick veneer		5,2 m	

Black combined the buoyant and dynamic forces and determined water velocities necessary to move flooded houses. Results are shown in Figure 2. Unanchored house may be moved by a combination of buoyant lifting and lateral water current movement. Anchorage is good insurance against total loss of the house (Black 1975). Black calculated that all of the studied houses could be completely submerged without floating if 3600 - 13600 kg of weight could be added. Black calculated the weight of different foundations: a concrete block foundation 5800 kg, a poured concrete foundation 7200 kg, a concrete block basement wall 14500 kg and poured concrete basement wall 24700 kg. Major difficulty with concrete block foundations is that the blocks tend to shear along the mortar joints (Black 1975).

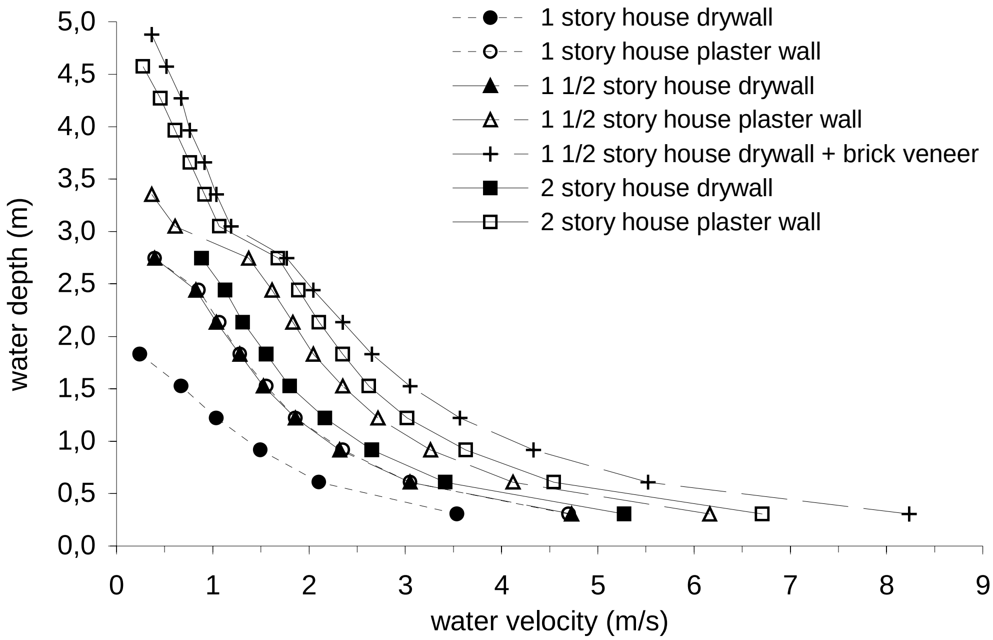

Figure 2 Water velocity necessary to move flooded house. Water flow directed against the length (9,8 m) of the house. (based on Black 1975)

Water flowing 1,8 m/s creates pressure of 1,7 kPa. Pressures as great as 1,7 kPa are very likely to cause structural damage to building components and severe erosion problems around the foundation. A good grass cover on an erosion resistant soil may safely stand higher velocities. Many soils upon which houses are built will not sustain velocity 1,5 m/s more than few hours. (Black 1975)

An allowable fibre stress of 6895 kPa is a common design value for common timber used in house construction. In buildings where the failure of a single piece is not considered to be as dangerous as in a house, an allowable fibre stress of 13790 kPa is used. The allowable bending moment for the 2 × 4 inch studs of the studied houses would be 347 Nm when using the lower fibre stress and 694 Nm when using the higher stress. (Black 1975)

Black calculated maximum bending moments produced by the dynamic and hydrostatic pressure (Figure 3). A water depth of 90 cm upon the studs would exceed the lower allowable bending moment even if there is no velocity. The higher limit is exceeded with water depth of 1,2 m with no velocity. A waterproof wall with openings sealed might withstand considerably more pressure than would be indicated by Figure 3 because occasionally pieces of common timber would not break until a fibre stress of 41000 to 55000 kPa were attained. When water enters a house the hydrostatic pressure equalises on both sides of the wall and is effectively cancelled. Figure 4 shows the dynamic pressure only. For example, when the water velocity is 2,4 m/s the lower allowable bending moment is exceeded at water depth of 1,0 m and the higher allowable bending moment at water depth of 1,6 m. (Black 1975)

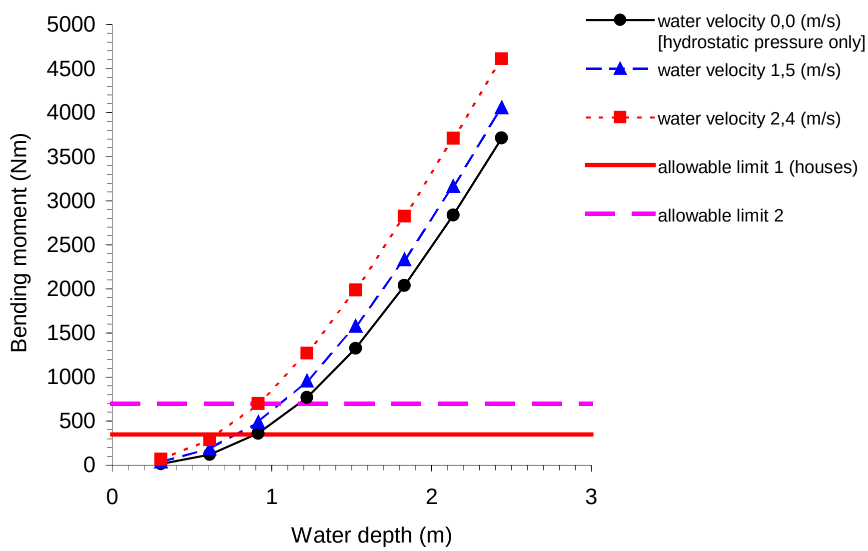

Figure 3 Bending moment produced by hydrostatic and dynamic pressure (based on Black 1975).

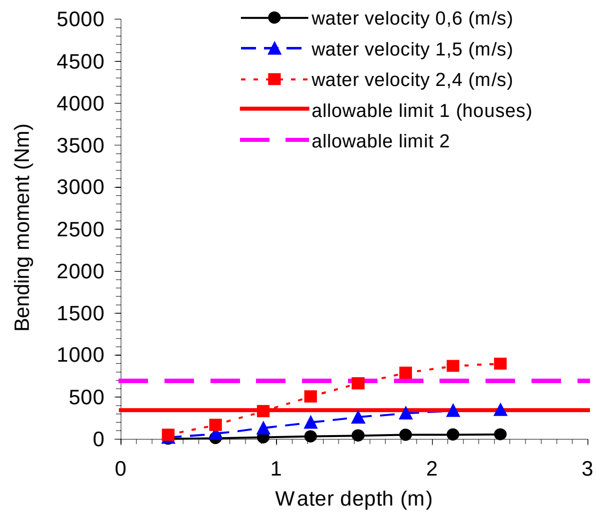

Figure 4 Bending moment produced by dynamic pressure (based on Black 1975).

Black calculated that a 20 cm thick and 2,4 m high concrete block wall fails under a moment of 280-330 Nm. A poured concrete wall is more than 10 times stronger and fails under a moment of 3900-4400 Nm. However concrete walls are frequently cracked and that is why they are also weaker. The water depth of 2,4 m would create a dangerous loading even if a perfectly poured concrete wall were assumed. (Black 1975)

2.4 DAMAGE CRITERION FOR BRICK AND MASONRY BUILDINGS BY CLAUSEN AND CLARK (1990)

Clausen and Clark (1990) developed criterion for predicting dam-break flood damages. They calculated water velocities v (m/s) and depths d (m) of Dale Dyke dam failure, UK 1864. The locations and damages of structures were determined from the details published by Harrison (1864). Clausen and Clark (1990) used the following damage categories:

Inundation: Damage similar to that caused by a natural low-velocity river flood. No immediate structural damage.

Partial damage: Moderate structural damage, i.e. windows and doors knocked out. Little damage to the major structural elements of the building.

Total destruction: Total structural collapse or major damage to the structure necessitating demolition and rebuilding.

The criterion of Clausen and Clark (1990) is presented in Figure 5. The boundaries between damage categories (inundation, partial damage, total destruction) can be delineated by curves of constant damage parameter vd (m^2/s). The boundary between inundation and partial damage is $vd = 3\ m^2/s$, the boundary between partial damage and total destruction is $vd = 7\ m^2/s$. Furthermore, partial damage or total destruction does not occur if $v < 2$ m/s. (Clausen and Clark 1990)

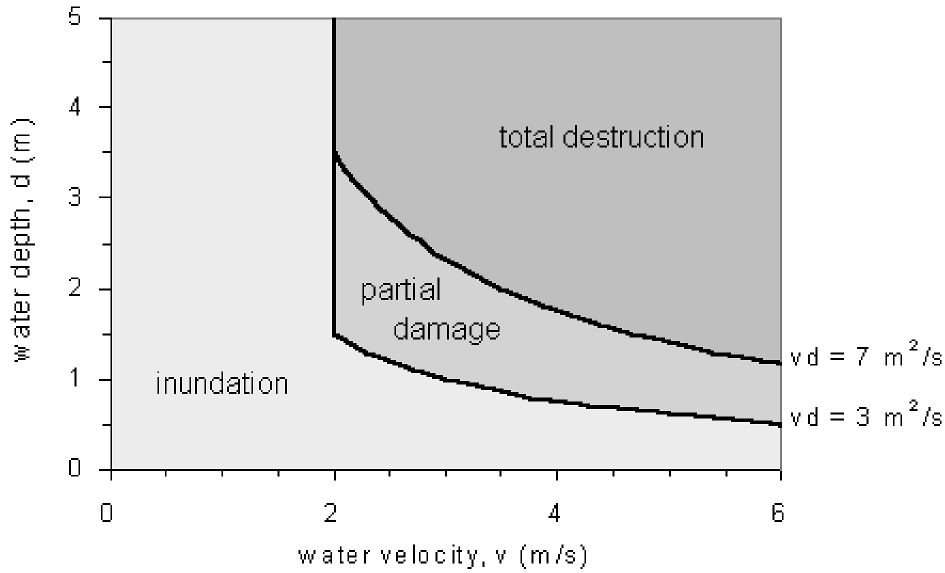

Figure 5 Damage criterion of brick and masonry buildings (based on Clausen & Clark 1990).

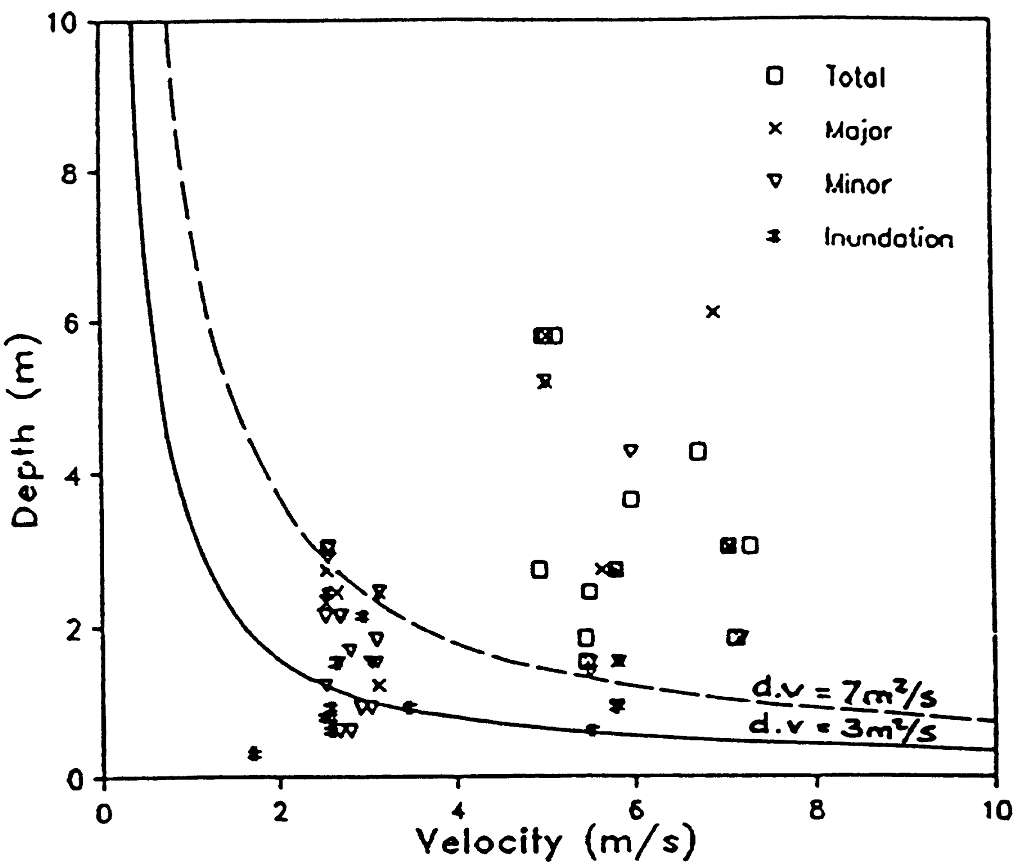

Figure 6 Building damage in Dale Dyke flood (Clausen & Clark 1990).

2.5 DESIGN ASPECTS OF BUILDINGS FOR FLOOD PLAIN LOCATIONS (LORENZEN ET AL. 1975)

Lorenzen et al. (1975) studied 15 farmsteads which had been flooded by Hurricane Agnes (1972) in four watersheds in the New York State area, USA. Each of these farmsteads had 1-4 buildings of interest to the survey. The buildings were classified as being wood framed, pole framed & masonry. Flood parameters (depth and velocity) were based on astute consideration of the remembrances of those who were present during the flood and evidence of high water marks. Depth of water was often marked on the side of the building. Velocity ranged up to 1,5 m/s at farmstead locations. (Lorenzen et al. 1975)

Lorenzen et al. calculated

1) general buoyancy of wood framed buildings
2) static and dynamic pressures
3) shock loads & impact force of debris.

Computations were made assuming that a building was not anchored to the foundation.

1) The buoyancy and floatation of sample buildings were calculated assuming that a building was not anchored to the foundation. The calculated floatation line of a typical 1-story building varied from the plate line to several feet above the plate line. In a 2-story building the floatation line was from the plate line to several feet below the plate line. Wood framed buildings and mobile homes tend to float in an upright position. An unanchored building may be displaced from it’s foundation long before full buoyancy is reached. Concrete items will not float, but tend to slide or roll. (Lorenzen et al. 1975)

2) Static pressure of the water has a high potential for displacement and destruction of basement walls if the wall is comparatively water tight. Pressures of water in the saturated soil around 1,8 m deep basement walls will build up to about 1800 kg/m^2 in the lower wall and under the floor. This is sufficient force to push the floor up until it cracks, or to buckle and breech the wall. Water and wind velocity pressures are compared in Figure 7. For the New York State area 50 year recurrence storm wind velocity is 31 m/s and 100 year recurrence storm wind velocity 31 m/s. It can be seen in Figure 7 that wind velocity 31 m/s and water velocity of 1,1 m/s cause equal pressure. A building frame strong enough to resist storm wind pressures has sufficient strength to resist also water velocity pressures. (Lorenzen et al. 1975)

3) Average impact forces of a floating log weighing 45 kg were calculated (Figure 7). A 90 kg log floating at a velocity 0,9 – 1,2 m/s could easily penetrate a board wall, snap a 2×4 inch stud or knock a hole in a unreinforced masonry wall. (Lorenzen et al. 1975)

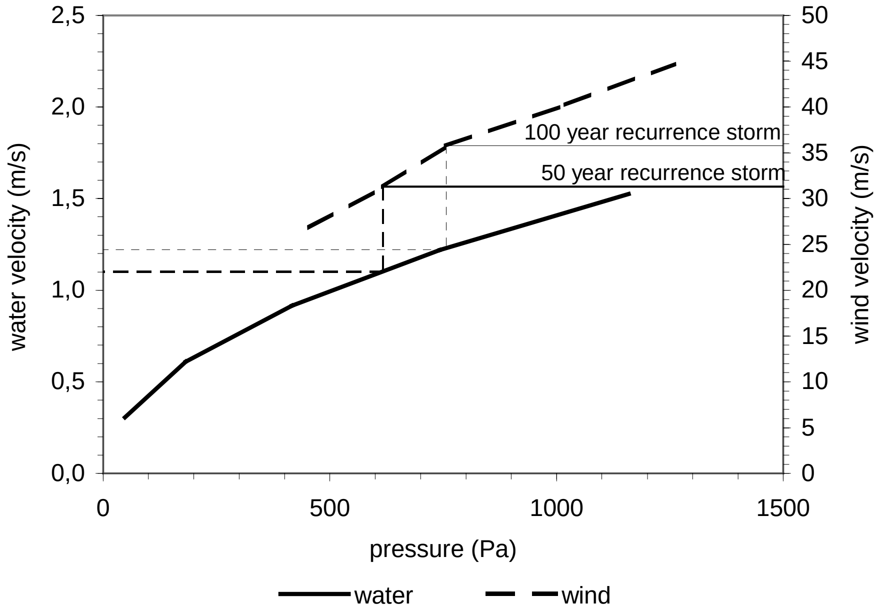

Figure 7 Comparison of water and wind velocity pressures (based on Lorenzen et al 1975).

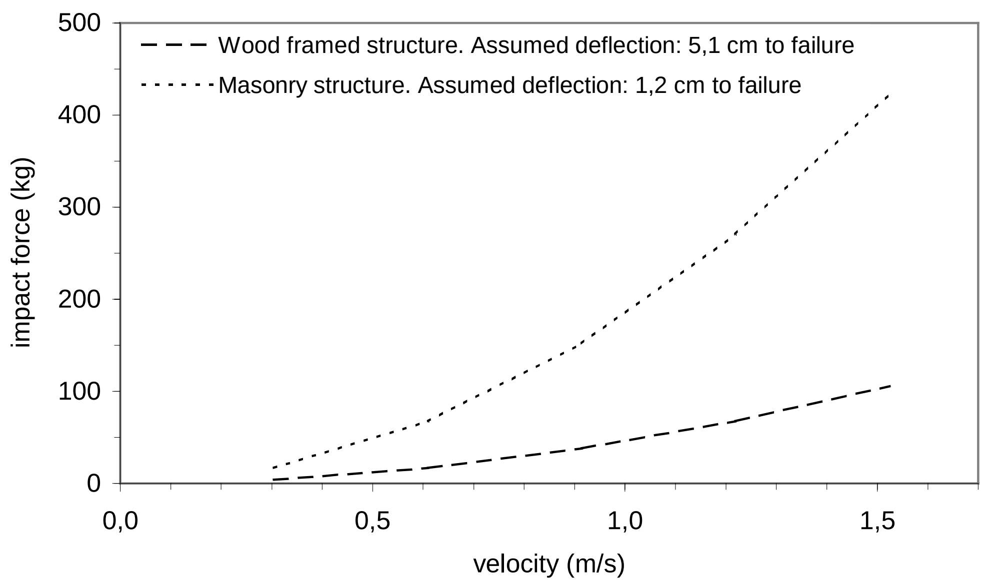

Figure 8 Impact forces of a floating log (based on Lorenzen et al. 1975).

Types and quality of construction and flood damage during the Hurricane Agnes flood in four watersheds, NY, USA (Lorenzen et al. 1975)

A) Pole type buildings, such as machine sheds and cold freestall barns survived without much damage. Flowing water may push off and floating debris may break some siding. The secure anchorage of the poles in the ground, the openness of the building and the laterally and crosswise bracing of the building tended to decrease the flood damage.

B) Traditional framed buildings on concrete foundations had considerable variance in regard to flood damage. Usually this type structure is quite watertight which means that water pressure may build up to a great degree. Major failures were found to be due to insufficient footings, such as rocks laid in a row and concrete without anchor bolts. Little damage was found if a building was well braced and anchored.

C) Concrete block construction resisted flood damage when supported on an adequate footing and not subjected to static water pressure. Several basement walls pushed in because water pressure was not permitted to equalise. Block footings were less stable than poured footings, and gave away in several instances.

D) Light steel framed buildings without insulation set on good footings and well anchored showed little flood damage. This type of buildings usually allow the equalisation of water pressure.

2.6 OTHER DAMAGE CRITERIA

According to Smith (1989), flow velocities larger than 2 m/s can cause damage or even collapse of buildings. Yet another damage criterion is presented in Figure 9. It illustrates the use of depth and velocity criteria to define low and high hazard floodplain locations. The criterion is based on New South Wales floodplain development guidelines (NSW Government 1986, ref. Smith 1991) and the high/low hazard definition includes other factors such as safety of residents during evacuation.

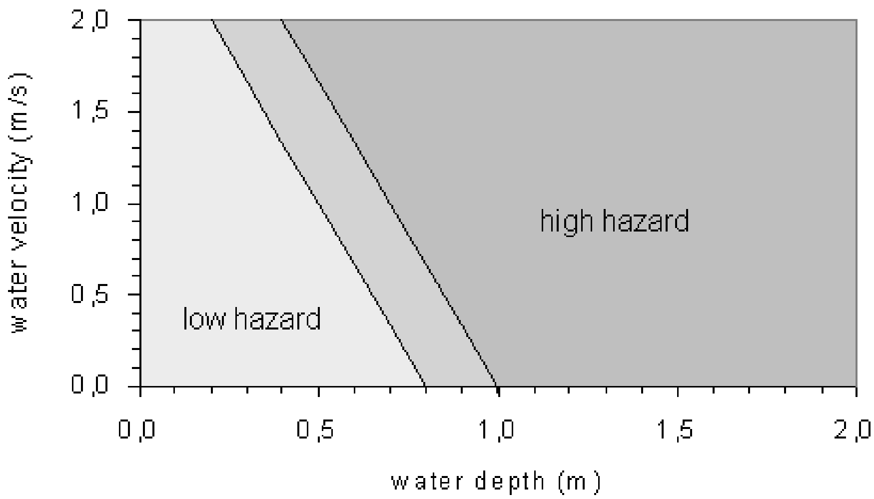

Figure 9 Hazard categories of building failure (includes factors such as safety of residents during evacuation) (NSW Government 1986, ref. Smith 1991).

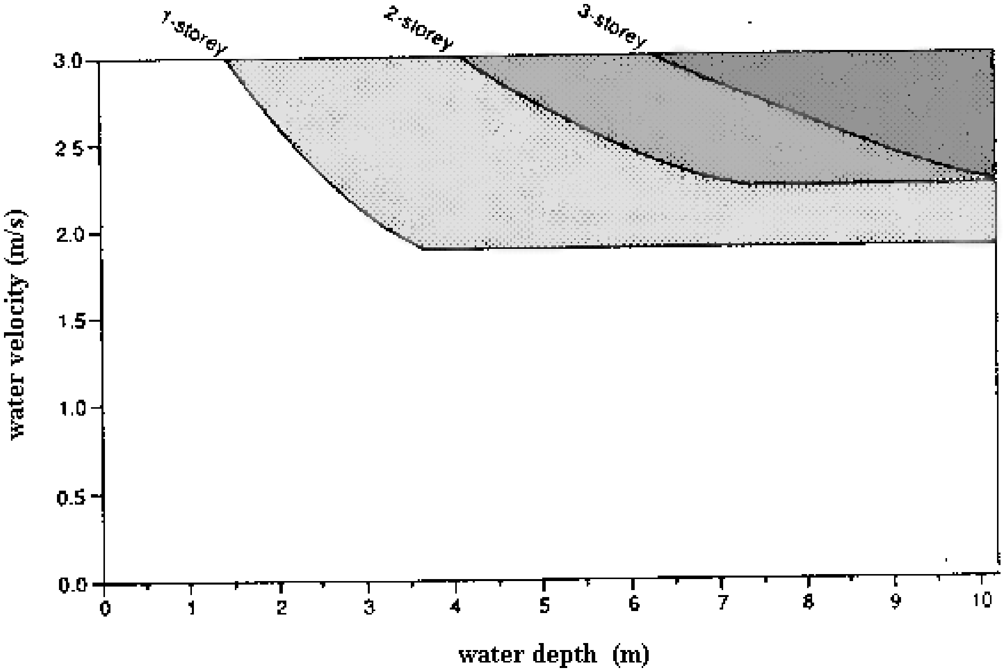

Figure 10 Critical water velocity and depth for the failure of masonry and concrete buildings (Smith 1991).

2.7 SUMMARY AND RECOMMENDATIONS

Several damage criteria for structures have been developed. Figure 11 compares the criterion of Sangrey et al. (1975) and the modified criterion of Black (1975). Sangrey et al. modified Black's criterion by chancing the hydraulic drag coefficient from value of one into two. Both criteria are developed mainly for timber-framed houses without anchorage. The Black's criterion is purely computational, whereas the criterion of Sangrey et al. is based on the analysis of flood event in a Chemung River flood plain. The Modified Black's criterion is more conservative than the criterion of Sangrey et al., especially with low water depth (small value of $(d - h_{fo})/10s$). The unmodified Black's criterion is even more conservative (Sangrey et al. 1975).

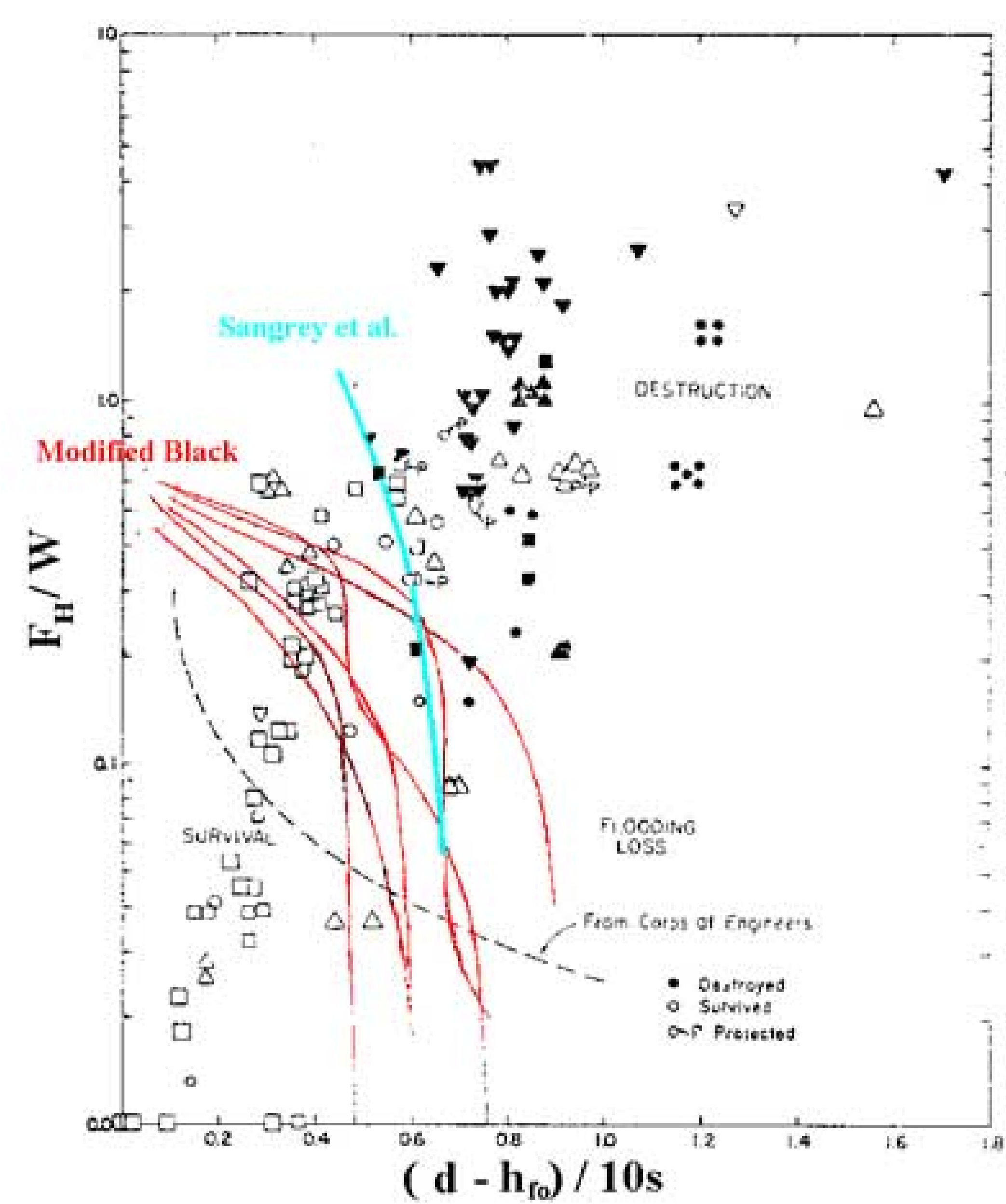

Figure 11 Comparison of two damage criteria for frame houses (based on Sangrey et al. 1975).

Figure 12 shows the comparison of the damage criterion of Black (1975) (unmodified) and of Clausen & Clark (1990). The damage criterion of Clausen & Clark is developed for masonry and brick structures and is based on the data of the Dale Dyke dam failure. The damage criterion of Clausen & Clark suggest that brick and masonry buildings withstand flooding better than timber-framed houses. In Figure 13 the damage criterion of Clausen and Clark is compared with the damage criterion proposed by Black (1975) and the US Army Corps of Engineers (USACE) for total structural damage of timber-framed houses. Both USACE and Clausen & Clark, and also the criteria presented by Smith (Figure 10) suggest that no structural damage occurs with velocities below about 2 m/s. The significant difference between 1-story and 2-story houses suggested by USACE was not detected from the data from Dale Dyke dam-break (Clausen & Clark 1990). The data of Sangrey et al. (1975) suggest that the USACE criterion for 2-story buildings is high (Clausen & Clark 1990).

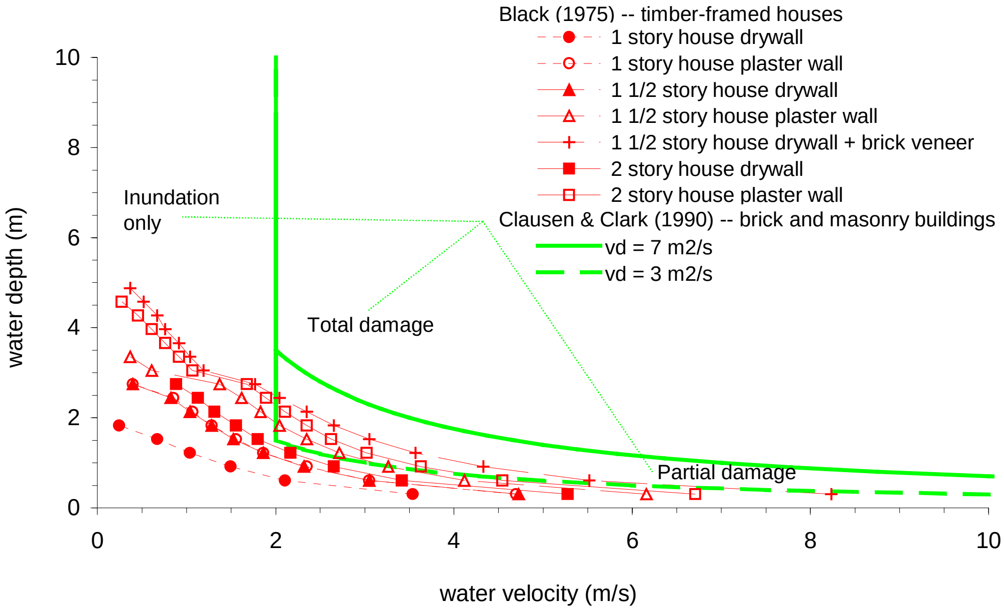

Figure 12 Comparison of damage criteria.

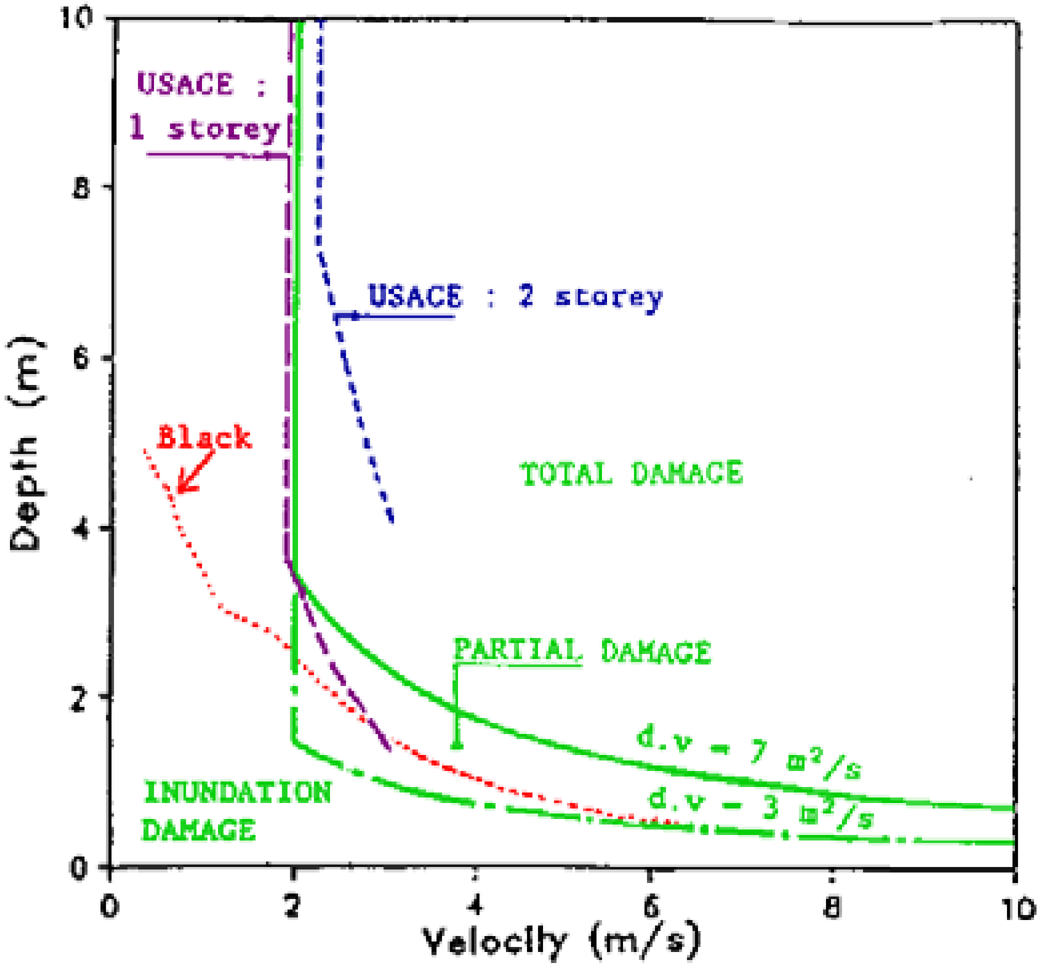

Figure 13 Comparison of three damage criteria (Clausen & Clark 1990).

Based on the studies described in chapter 2 a recommendation for the Finnish houses is given in Table 3 which introduces the flow conditions causing structural damage, either total or partial.

Table 3 Recommended damage parameters for structural damage of Finnish houses.

house type	**partial damage**	**total damage**
wood-framed		
unanchored	$vd \geq 2$ m^2/s	$vd \geq 3$ m^2/s
anchored	$vd \geq 3$ m^2/s	$vd \geq 7$ m^2/s
masonry, concrete & brick	$v \geq 2$ m/s & $vd \geq 3$ m^2/s	$v \geq 2$ m/s & $vd \geq 7$ m^2/s

3. THE MANNING'S ROUGHNESS COEFFICIENT OF FOREST AND HOUSES

3.1 ROUGHNESS

"**Roughness** — A term used by hydraulic engineers and hydrologists designating a measurement or estimate of the resistance that streambed materials, vegetation, and other physical components contribute to the flow of water in the stream channel and floodplain. It is commonly measured as the Manning’s roughness coefficient." (Water Words Dictionary 2000)
"**Roughness Coefficient** — (Hydraulics) A factor in velocity and discharge formulas representing the effect of channel roughness on energy losses in flowing water." (Water Words Dictionary 2000)

The most common way to calculate the flow velocities is the Manning - Strickler - formula

$$v = 1/n \cdot R^{2/3} \cdot I^{1/2}$$

Equation 2

where v is flow velocity (m/s), M = 1/n is the Manning - Strickler – coefficient ($sm^{-1/3}$), R is the hydraulic radius (m) and I is the slope (m/m). (Mertens 1994, Chow 1973)

The reason why the Manning formula is so widely used is its simplicity. Besides it gives satisfactory results to practical applications. As a criticism it can be said that the derivation of formula involves approximations, especially in the exponent of R, and there are uncertainties in the dimensions of n. For selecting the n value there is no exact method, although there exist tables and pictures of typical n values for channels of various types. (Chow 1973)

3.2 HYDRAULIC SCALE MODELS

In the RESCDAM study physical hydraulic scale models were used to study the Manning's roughness coefficient of forest and houses.

"The term **model** is used in hydraulics to describe the simulation of a 'prototype', i.e. field size, situation." (Novak & Kabelka 1981)

"**Model** — (1) (General) An idealized representation of reality developed to describe, analyze, or understand the behavior of some aspect of it." (Water Words Dictionary 2000)

Hydraulic models — "Any physical model for the simulation of flow processes, flow states and events, which concern problems of hydraulic engineering or technical hydromechanics." (Kobus 1980)

In general, the model and the prototype must be dynamically similar which means that:
– The motion paths are geometrically similar.
– The distances in relation to the time are kinematically similar.
– The forces are dynamically similar.
The results obtained from the model can be interpreted with the help of model laws. These laws can be derived from the dimensions of basic magnitudes. (Kuuskoski 1948)

For flows under the influence of gravity (e.g. free surface flows) the geometrical similarity and equality of the Froude number Fr in model and prototype are required (Kobus 1981). When investigating the similarity under the exclusive or overwhelming action of gravity we accept geometric similarity and neglect other forces, such as frictional resistance of a viscous liquid, capillary forces, the forces of volumetric elasticity and cavitation phenomena on the basis of mechanical similarity (Kuuskoski 1948).

The condition of the equal flow regime in the model and in prototype must be added to the analysis of similarity based on prevailing forces. For example, in laminar flow the hydraulic gradient changes with the first power, but in fully developed turbulent flow with the square of velocity. In the prototype the flow is usually turbulent and therefore the model must not be so small that the flow regime changes into laminar flow. The criterion for turbulent and laminar flow in open channels and also in pipes is the Reynolds number. Laminar flow in wide open channels occurs when Reynolds number is smaller than the critical Reynolds number Re_{cr} = 2100. (Novak and Cábelka 1980)

According to the Froude model law, the velocity (v) relation between the model and the prototype is

$$v_r = \frac{v_p}{v_m} = \frac{\sqrt{l_p}}{\sqrt{l_m}} = l_r^{1/2}$$

Equation 3

where l = length
subscript p stands for prototype
subscript m stands for model
subscript r stands for ratio.
l_r = scale number of lengths

The relation between discharges (Q) is

$$Q_r = \frac{Q_p}{Q_m} = \frac{A_p v_p}{A_m v_m} = \frac{l_p^2 \cdot \sqrt{l_p}}{l_m^2 \cdot \sqrt{l_m}} = l_r^{5/2}$$

Equation 4

where A = area

The relation between times (t) is

$$t_r = \frac{t_p}{t_m} = \frac{l_p \sqrt{l_m}}{l_m \sqrt{l_p}} = \frac{l_p^{1/2}}{l_m^{1/2}} = l_r^{1/2}$$

Equation 5

The relation between forces (F) is

$$F_r = \frac{F_p}{F_m} = \frac{l_p^3}{l_m^3} = l_r^3$$

Equation 6

The relation between pressures (p) is

$$p_r = \frac{p_p}{p_m} = \frac{l_p}{l_m} = l_r$$

Equation 7

3.3 ROUGHNESS OF FOREST

3.3.1 Facility and tree models

The test facility was a 50 m long, 1,1 m wide and 1,3 m deep rectangular fixed bed flume. The water amount circulating in the flume was measured with a triangular weir. As a foundation for tree models perforated plywood boards (thickness 5,5 cm, length 3,35 m and hole diameter 32 mm) were mounted horizontally on the bottom of the flume. The plywood boards were also used as slopes upstream and downstream the saplings of Norway spruce and birch to stabilise flow and cause turbulence. The vertical plywood board was placed in the beginning of flume to create mixing effect, besides that the floating horizontal boards reduced heaving in the flume. The water depth was controlled with an overflow weir situated downstream. The weir heights of 15 cm, 30 cm and 45 cm were used.

The saplings of Norway spruce and birch, which are the most common tree types in Finland, were used as tree models. The heights of spruce saplings varied from 56,0 cm to 72,0 cm. The trunk diameters were between 1,2 and 1,6 cm and the maximum width of the saplings were from 29 cm to 52 cm. The heights and diameters of white birch were not measured for the study. Because the tests were conducted in the early spring, the birches were maintained indoors in order to propagate the leaves. All the plants were mounted into the holes of plywood board with flexible fastening, which allowed the saplings to bend from their foundation. The whole test facility for both vegetation tests is presented in Figure 14.

The head loss caused by saplings was determined by measuring water table upstream and downstream the saplings. While studying the spruce saplings the manual point gauges were used to measure the water levels. When studying the birch saplings a differential pressure transducer was used to measure the difference in water level and a pressure sensor to measure the water depth. The differential pressure transducer and the pressure sensor were used while studying roughness of houses, and the system is depicted in chapter 3.4.1 and Figure 26.

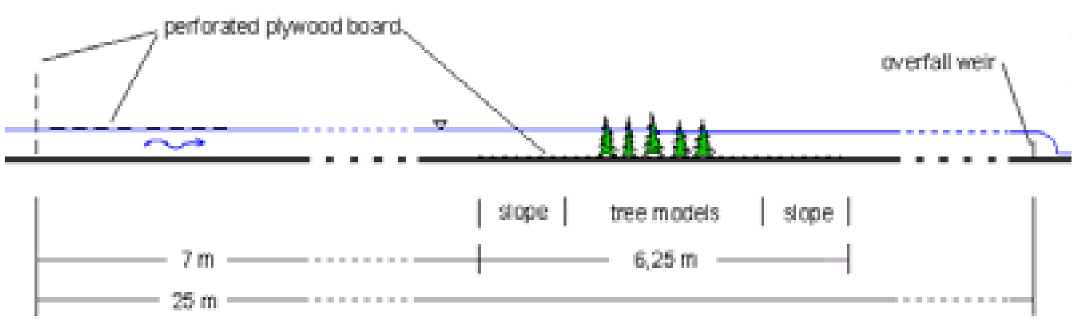

Figure 14 The test arrangement for studying the roughness of forest in the fixed bed flume.

Figure 15 Examples of Norway spruce and birch saplings used as tree models.

3.3.2 Experimental procedure

13 different sapling compositions, the scale model forests, were studied. These are presented in Table 4 and Figure 16. All scale model forests were studied with spruce saplings and scale model forests A, B, B3, C, F and H were used with birch saplings. Scale model forests B and D2 were studied also with spruce saplings which low branches were removed. These experiments are denoted with codes Bk10, Bk15, D2k10 and D2k15. In tests Bk10 and D2k10 low branches were removed up to 10 cm height and in Bk15 and D2k15 low branches were removed up to 15 cm height.

Discharges from 23 l/s to 160 l/s and water depths from 15 to 58 cm were used. Using equation $v = Q/(d \cdot b)$, where *v* = velocity, *Q* = discharge, *d* = average water depth and *b* = width of the flume, the average velocities varied from 8 to 52 cm/s using. Flow velocities were not measured. Water depth was controlled with the overflow weir situated downstream. The weir heights of 15 cm (low), 30 cm (medium) and 45 cm (high) were used. Most of the scale model forests were tested with all three weir heights. From three to six different discharges were used with each weir height.

Table 4 Studied scale model forests.

model forest	code	number of saplings	number of rows	number of saplings in a row: 1st row	2nd row	3rd row	4th row	5th row	6th row	distance between rows (cm)	distance between saplings in a row (cm)	studied tree models: spruce	birch
square	A	15	5	3	3	3	3	3		40	40	yes	yes
rows													
96 cm	B4	9	3	3	3	3				96	40	yes	no
80 cm	B	9	3	3	3	3				80	40	yes	yes
56 cm	B2	9	3	3	3	3				56	40	yes	no
32 cm	B3	9	3	3	3	3				32	40	yes	yes
argyle	C	15	6	3	2	3	2	3	2	32	40	yes	yes
random													
15 saplings	D1	15										yes	no
9 saplins	D2	9										yes	no
line													
middle	F	5	5	1	1	1	1	1		40		yes	yes
side	G	5	5	1	1	1	1	1		40		yes	no
row													
3 saplings	H	3	1	3							40	yes	yes
2 saplings	I	2	1	2							40	yes	no
single	J	1	1	1								yes	no

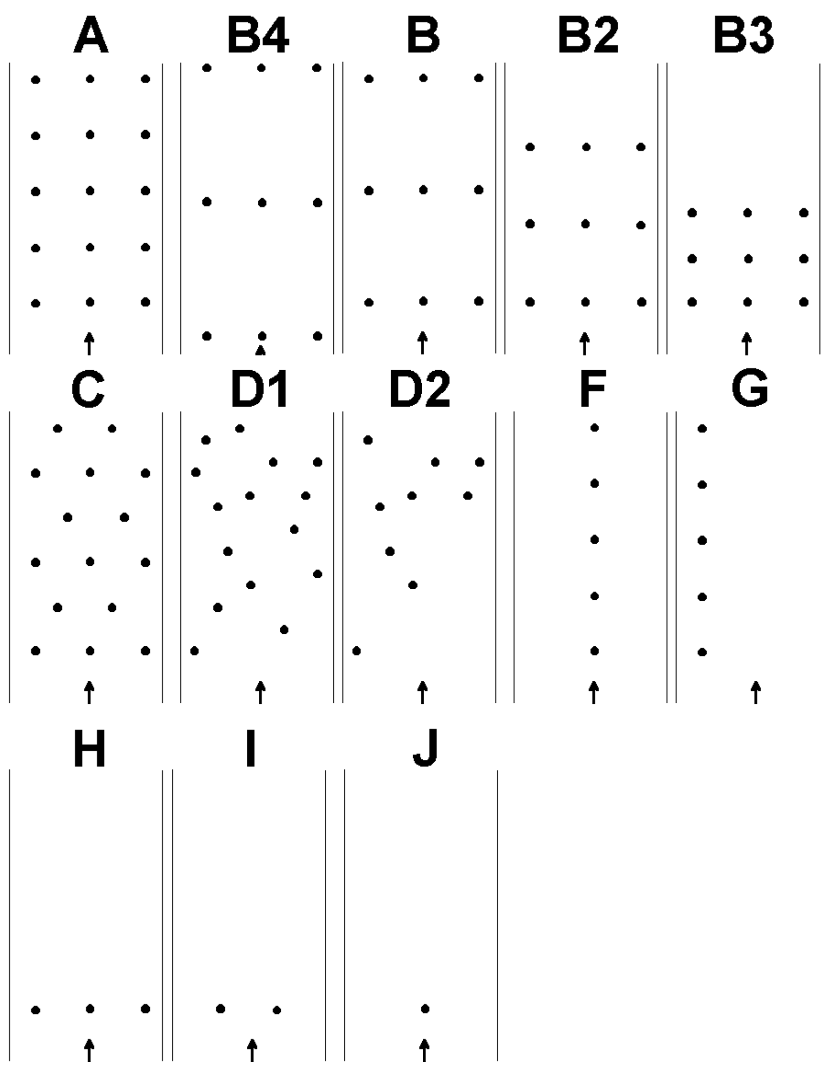

Figure 16 Studied scale model forests.

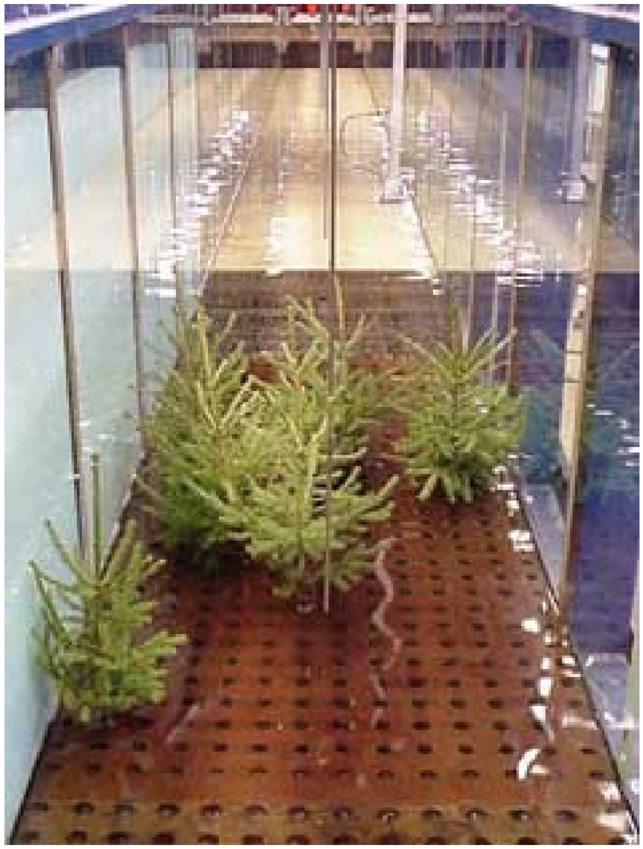

Figure 17 Spruce saplings (model forest D2) mounted into the holes of the plywood board.

Figure 18 Spruce sapling forest B2, Q = 59 l/s, d = 49 cm.

Figure 19 Spruce sapling forest D1, Q = 161 l/s, d = 42 cm.

Figure 20 Birch sapling forest C, Q = 133 l/s, d = 54 cm.

3.3.3 Results

Spruce and birch sapling forests were tested with different discharges and water depths as described in chapter 3.3.2. For each test the difference in water level upstream and downstream the saplings Δd_m was measured. Results for the scale model forest A are presented in Figure 21. Also the difference in water level in the flume without saplings Δd_e was measured with same discharges and weir heights as the sapling forests. Sapling forests A, B, B2, B3, B4, C, D1 and D2 were then chosen for further analysis.

Using the Manning-Strickler-formula (Equation 2) $v = 1/n \cdot R^{2/3} \cdot I^{1/2}$ the Manning's roughness coefficients of the saplings were calculated. The hydraulic radius $R = (d \cdot b)/(2 \cdot d + b)$ and velocity $v = Q/(d \cdot b)$ in the Manning-Strickler-formula were calculated using the water depth d which was an average of depth upstream the saplings and downstream the saplings. The effect of the flume was removed by using the slope $I = (\Delta d_m - \Delta d_e)/l_f$ in the Manning-Strickler-formula, where the l_f is the length of the sapling forest. This means that the calculated Manning's n presents the roughness of the saplings without the effect of the flume bottom. Calculated Manning's n for the scale model forest A is presented in Figure 22.

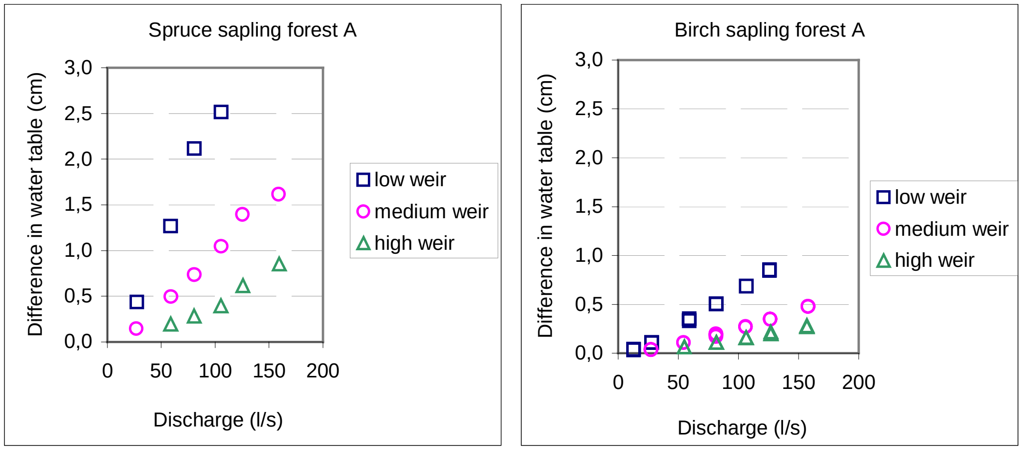

Figure 21 Difference in water table in the case of the scale model forest A.

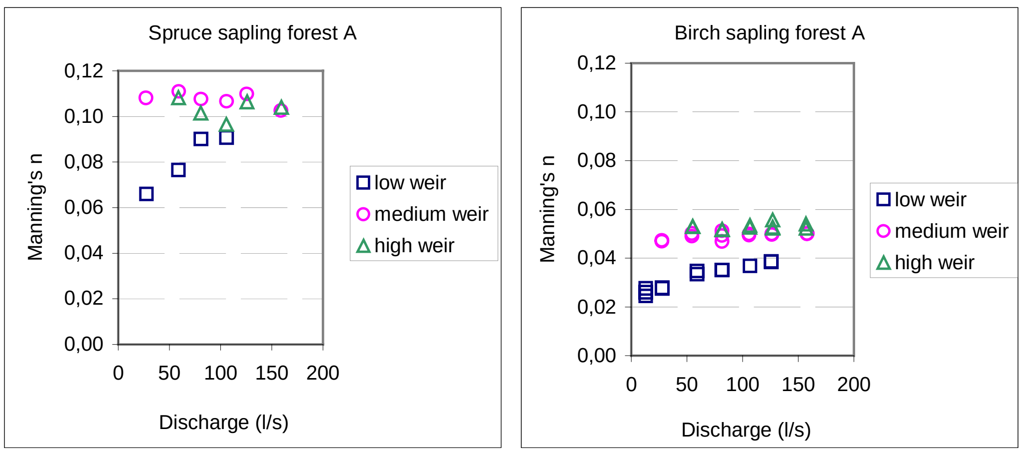

Figure 22 Manning's *n* of the scale model forest A.

The areas of the model forests A_f (m^2) were determined. The densities of the forests S_f, trees per square metre (tr/m^2) were then calculated. The trunk diameter and height of the spruce saplings were measured before the experiments. The trunk volumes of the saplings V_{tr} (m^3) were then calculated. Because the dimensions of the birch saplings were not measured, the trunk volumes of the spruce saplings were used to estimate the trunk volumes of the birch saplings. The trunk volumes of the model forests $V_f = V_{trav} \cdot S_f$ (m^3/m^2) were calculated using the average trunk volume of the saplings V_{trav}. Based on the water depth data, the submerged trunk volumes V_{fsub} of the model forests were calculated for each experiment.

The measured and calculated parameters characterising the scale model trees and forests and the flow were scaled according to the Froude model laws using the scale numbers 5, 10 and 20. The summary of the parameters is presented in tables Table 5, Table 6 and Table 7.

Table 5 The summary of flow parameters.

	FLOW								
	flow depth d			flow velocity v			velocity times depth vd		
	min.	max.		min.	max.		min.	max.	
scale model	15	58	cm	8	52	cm/s	245	1459	cm^2/s
5x scaled	0,7	2,9	m	0,2	1,2	m/s	0,3	1,6	m^2/s
10x scaled	1,5	5,8	m	0,3	1,6	m/s	0,8	4,6	m^2/s
20x scaled	3,0	11,6	m	0,4	2,3	m/s	2,2	13,1	m^2/s

Table 6 The summary of tree parameters.

	TREE							
	average height h_{tr}		average max. width w_{tr}		average trunk diameter $ø_{tr}$		average trunk volume V_{tr}	
scale model	62	cm	37	cm	1,3	cm	70	cm^3
5x scaled	3,1	m	1,9	m	0,07	m	0,01	m^3
10x scaled	6,2	m	3,7	m	0,13	m	0,07	m^3
20x scaled	12,4	m	7,4	m	0,27	m	0,56	m^3

Table 7 The summary of forest parameters.

	FOREST A, B, B2, B3, B4, C, D1 & D2											
	area A_f			density S_f			trunk volume V_f			submerged trunk volume V_{fsub}		
	min.	max.		min.	max.		min.	max.		min.	max	
scale model	1	3	m^2	2,8	8,5	tr/m^2	199	596	cm^3/m^2	48	541	m^3/m^2
5x scaled	26	79	m^2	1136	3409	tr/ha	10	30	m^3/ha	2	27	m^3/ha
10x scaled	106	317	m^2	284	852	tr/ha	20	60	m^3/ha	5	54	m^3/ha
20x scaled	422	1267	m^2	71	213	tr/ha	40	119	m^3/ha	10	108	m^3/ha

The calculated Manning’s roughness coefficients were scaled according to the Froude model law using scale numbers 5, 10 and 20. The three different scale model forests (spruce, spruce without low branches and birch) were approached separately but the data of all the three scales (5, 10 and 20) were combined. The relationships between Manning's n and water depth d (m), velocity times depth vd (m^2/s) and submerged trunk volume V_{fsub} were studied. The scaled data is depicted in figures Figure 23 – Figure 25, each figure including 5x-, 10x- and 20x-scaled data.

Figure 23 approaches the relation between the Manning's roughness coefficient n and the water depth d. It can be seen that the increase of water depth means greater values of n. In the three upper graphs the data is divided into two or three different velocity categories. The clear effect of velocity categories can be discovered only in the data of spruces without low branches. The lower velocities causes the largest values of Manning's n. In the lower three graphs the data is divided into two categories according to forest density. In all the three types of experiments the roughness increases when the density of the forest increases.

In Figure 24, the roughness coefficient n and the flow velocity times flow depth vd are plotted. Larger values of vd generally mean greater values of n, but the effect is not as clear as in the case of d (Figure 23). Again the larger values of roughness are attained with the greater densities of forest (lower graphs) or water depths (upper graphs).

Figure 23 illustrates the relation between the Manning's roughness coefficient n and the submerged trunk volume of the forest V_{fsub}. There is a clear connection between n and V_{fsub}:

bigger values of V_{fsub} mean greater values of *n*. In addition, larger densities of forest cause the biggest values of *n*.

Figures 23, 24 and 25 can be used to estimate the Manning's roughness of forest. While estimating the roughness of coniferous forest the appropriate way is to use the results of the spruce sapling experiments. The roughness of deciduous forest is evaluated best by using the birch sapling experiments. Note that the Manning's *n* in figures 23, 24 and 25 describes the roughness of the trees but the bottom roughness caused by wood soil, undergrowth, stones, etc. is not included.

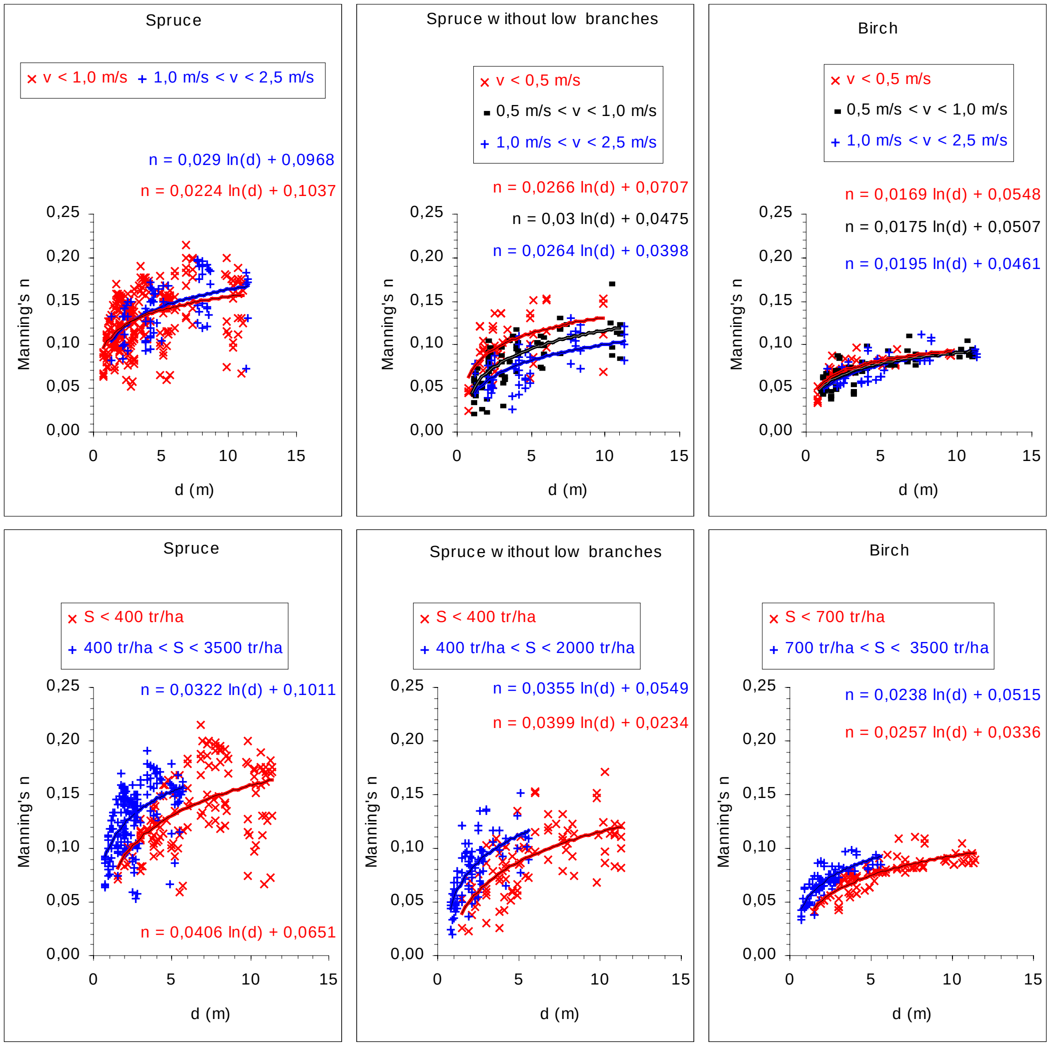

Figure 23 The Manning's *n* of forest as a function of flow depth *d* (m).

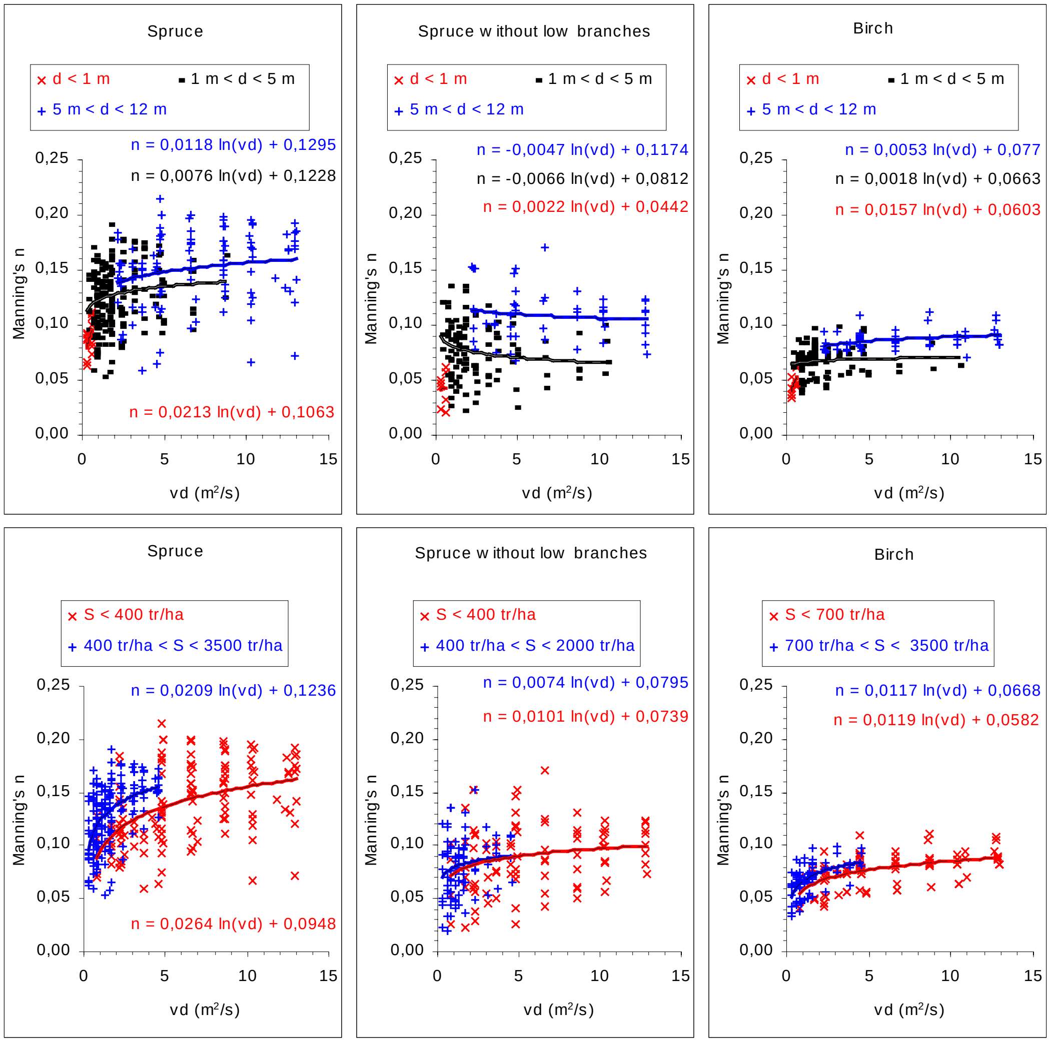

Figure 24 The Manning's *n* of forest as a function of flow velocity times flow depth *vd* (m^2/s).

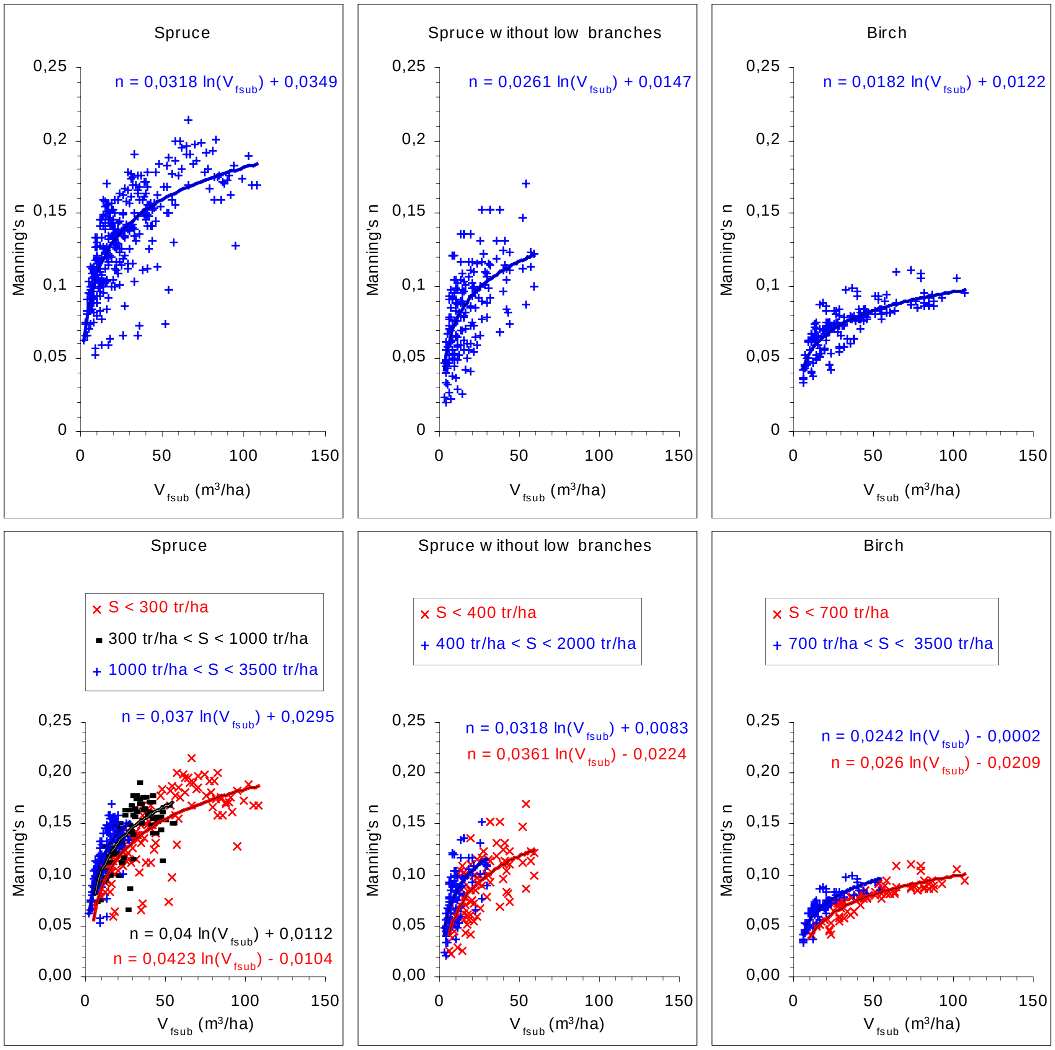

Figure 25 The Manning's *n* of forest as a function of submerged trunk volume V_{fsub} (m^3/ha).

3.4 ROUGHNESS OF HOUSE GROUPS

3.4.1 Facility

Roughness of houses was studied in the fixed bed flume. Test arrangements are presented in Figure 26. The facility was almost the same as in the study of the forested area. A differential pressure transducer and the pressure sensor were used to measure the difference in water level and the water depth.

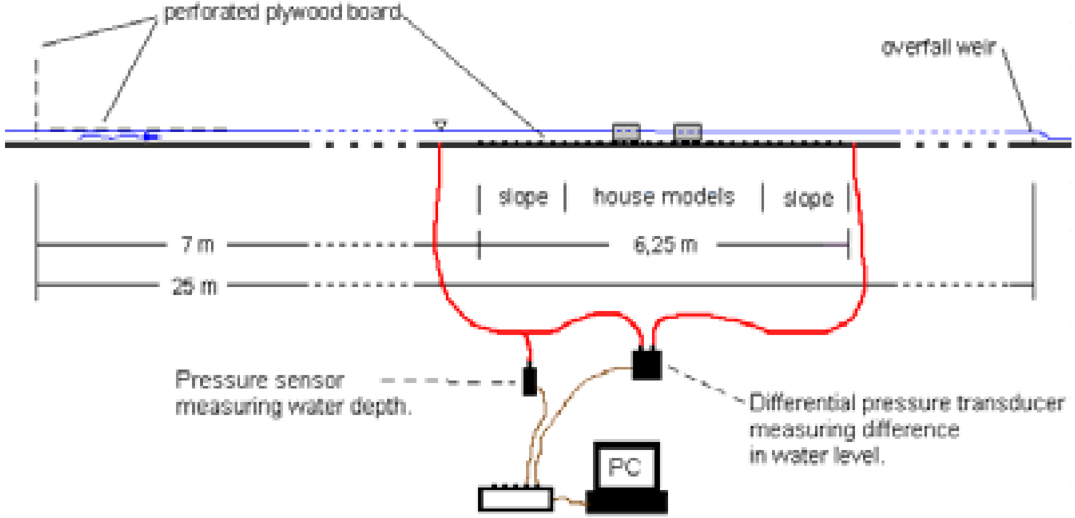

Figure 26 The test arrangement for studying the roughness of houses in the fixed bed flume.

3.4.2 Experimental procedure

The scale model houses used in the experiment were 34,5 cm long and 26,0 cm wide. Eight different house groups, depicted in Figure 27, were tested. Six groups (A, C, D, G, H and I) had houses situated lengthways in the flume. Groups A, C and D had three rows of houses and groups G, H and I two rows. There were two adjacent houses in each row and the space between houses was 26,5 cm. The space between rows were in groups A and G 34,5 cm, in groups C and H 69 cm and in groups D and I 103,5 cm. Diagonally situated houses were tested in groups E and F, which consisted of three rows of houses and the space between rows was 34,5 cm in group E and 69 cm in group F. From five to eight different discharges from 5 l/s to 37 l/s were used with each group.

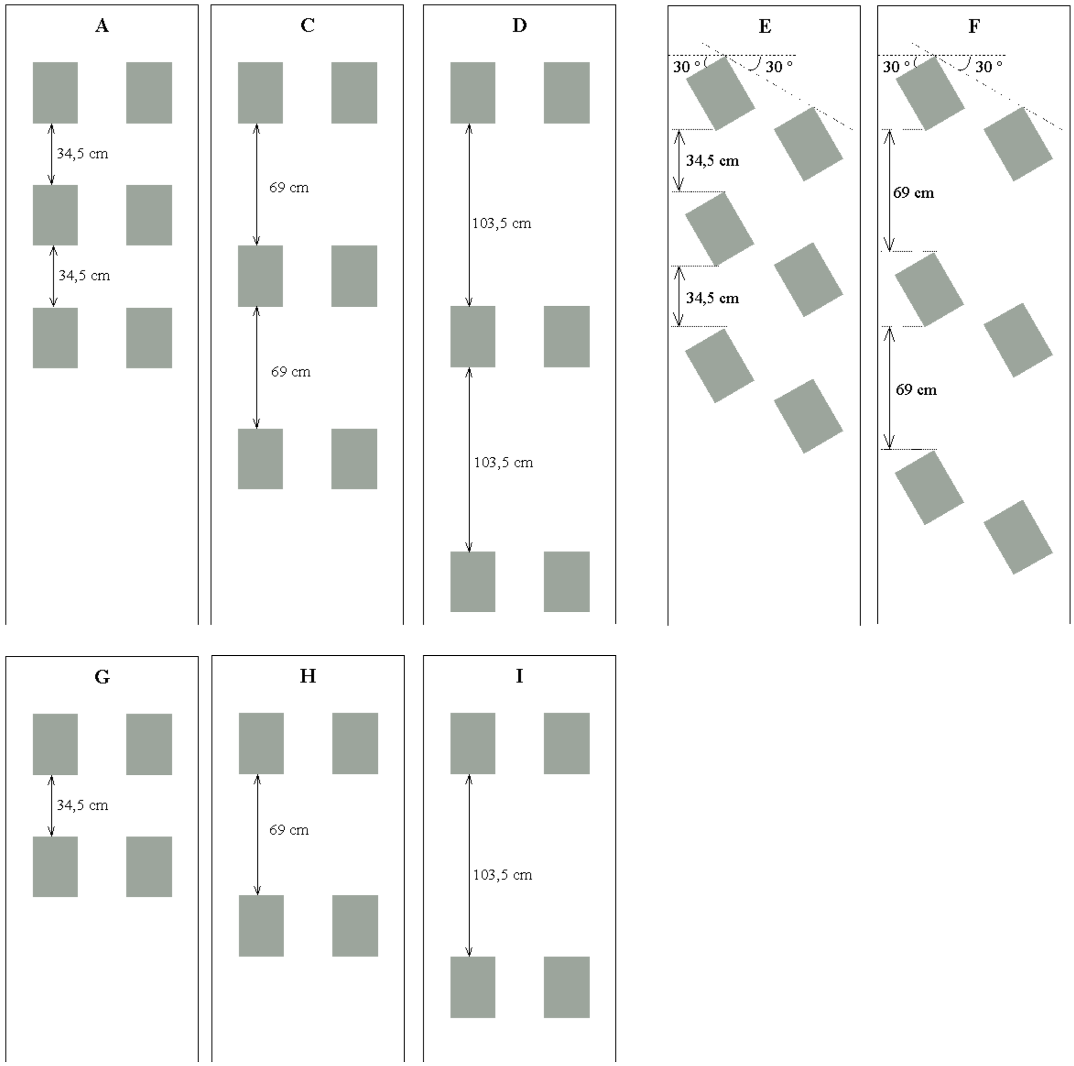

Figure 27 Tested groups of houses.

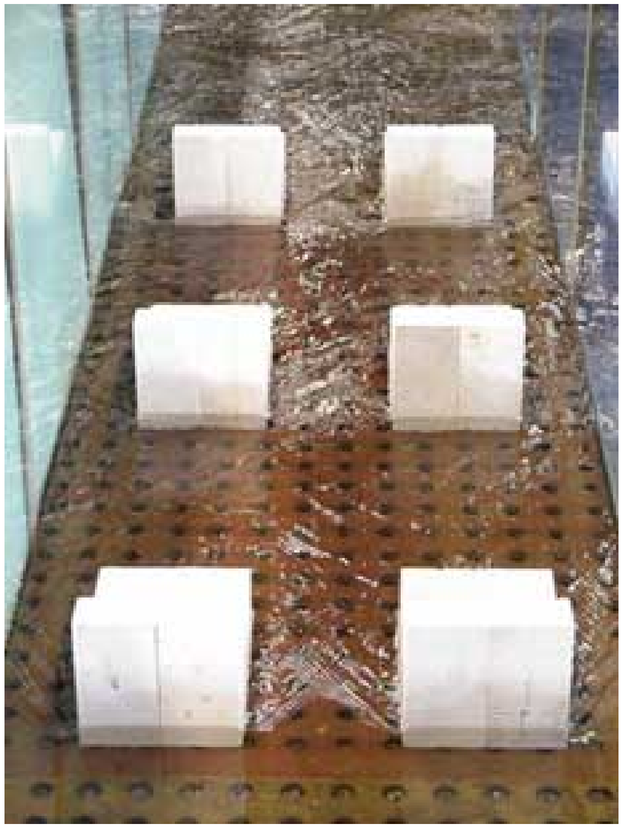

Figure 28 Water flowing through the scale model house group C, Q = 13 l/s, $d_{average}$ = 5,5 cm.

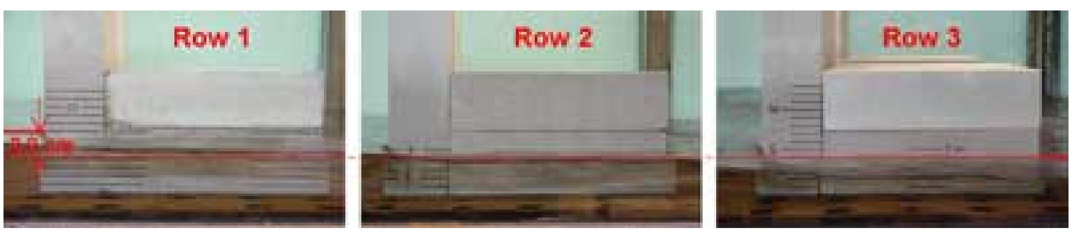

Figure 29 The scale model house group C, Q = 13 l/s.

3.4.3 Results

Scale model house groups were tested with different discharges as described in chapter 3.4.2. For each test the difference in water level upstream and downstream the house model group Δd_m was measured. In Figure 30 the results for the scale model house group A are presented. Also the difference in water level in the flume without scale model houses Δd_e was measured.

Using the Manning-Strickler-formula (Equation 2) $v = 1/n \cdot R^{2/3} \cdot I^{1/2}$ the Manning's roughness coefficients n of the scale model house groups were calculated. The hydraulic radius $R = (d \cdot b)/(2 \cdot d + b)$ and the velocity $v = Q/(d \cdot b)$ were calculated separately upstream (R_1, v_1) and downstream (R_2, v_2) the house models and using the width of the flume b. In the Manning-Strickler-formula the average values of hydraulic radius and flow velocity, $R = (R_1 + R_2)/2$ and $v = (v_1 + v_2)/2$, were used. Flow velocities were not measured. The effect of the flume was removed using $\Delta d_m - \Delta d_e$ as the difference in water level when calculating the slope I in the Manning-Strickler-formula. This means that the calculated

Manning's *n* presents the roughness of the scale model houses without the effect of the flume bottom. Calculated Manning's *n* for the scale model house group A is presented in Figure 30.

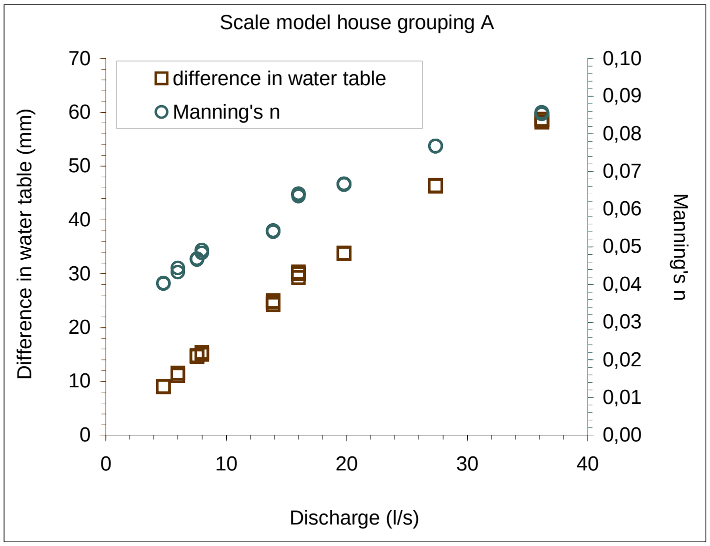

Figure 30 Difference in water table and the Manning's *n* of the scale model house group A.

The parameters characterising the scale model houses and the house groups are presented in Table 8. The width of the scale model houses w_h was 0,26 m, the length l_h 0,345 m and the area A_h= 0,09 m^2. There were four or six scale model houses in each tested group, which means the total area of houses A_{hsum} either 0,36 m^2 (4A_h) or 0,54 m^2 (6A_h). The area of groups A_g varied from 1,5 to 4,6 m^2, building coverage was A_{hsum}/A_g = 0,12 – 0,24 m^2/m^2 and the number of houses per square metre S_g = 1,3 – 2,6 houses/m^2. Three scaling factors 30, 40 and 50 were chosen and the scaled parameters are presented in Table 9. Note the unit of the scaled building coverage parameter A_{hsum}/A_g m^2/ha and S_g houses/ha. The parameters characterising the flow in the scale model experiments and the scaled flow parameters are presented in Table 10.

Table 8 Parameters characterising the scale model houses and house groups.

SCALE MODEL EXPERIMENTS													
	house			house group									
Scale model house group	width w_h (m)	length l_h (m)	area A_h (m^2)	num. of rows	num. of houses	total area of houses A_{hsum} (m^2)	Distance between houses (m) ↓	→	width w_g (m)	length l_g (m)	area A_g (m^2)	A_{hsum}/A_g (m^2/m^2)	S_g (houses/m^2)
A	0,26	0,345	0,09	3	6	0,54	0,35	0,26	1,1	2,1	2,3	0,24	2,6
C	0,26	0,345	0,09	3	6	0,54	0,69	0,26	1,1	3,1	3,4	0,16	1,8
D	0,26	0,345	0,09	3	6	0,54	1,04	0,26	1,1	4,1	4,6	0,12	1,3
G	0,26	0,345	0,09	2	4	0,36	0,35	0,26	1,1	1,4	1,5	0,24	2,6
H	0,26	0,345	0,09	2	4	0,36	0,69	0,26	1,1	2,1	2,3	0,16	1,8
I	0,26	0,345	0,09	2	4	0,36	1,31	0,26	1,1	2,8	3,0	0,12	1,3
E	0,26	0,345	0,09	3	6	0,54	0,35	0,26	1,1	2,3	2,6	0,21	2,3
F	0,26	0,345	0,09	3	6	0,54	0,69	0,26	1,1	3,4	3,7	0,15	1,6

Table 9 Parameters characterising the scaled houses and house groups.

SCALED	**scaling factor**		**30**										
	house			**house group**									
Scale model house group	width w_h (m)	length l_h (m)	area A_h (m^2)	num. of rows	num. of houses	total area of houses A_{hsum} (m^2)	Distance between houses (m) ↓	→	width w_g (m)	length l_g (m)	area A_g (m^2)	A_{hsum}/A_g (m^2/ha)	S_g (houses/ha)
A	7,8	10,4	81	3	6	484	10,4	7,8	33	62	2049	2364	29
C	7,8	10,4	81	3	6	484	20,7	7,8	33	93	3074	1576	20
D	7,8	10,4	81	3	6	484	31,1	7,8	33	124	4099	1182	15
G	7,8	10,4	81	2	4	323	10,4	7,8	33	41	1366	2364	29
H	7,8	10,4	81	2	4	323	20,7	7,8	33	62	2049	1576	20
I	7,8	10,4	81	2	4	323	39,2	7,8	33	83	2732	1182	15
E	7,8	10,4	81	3	6	484	10,4	7,8	33	70	2298	2108	26
F	7,8	10,4	81	3	6	484	20,7	7,8	33	101	3323	1458	18

SCALED	**scaling factor**		**40**										
	house			**house group**									
Scale model house group	width w_h (m)	length l_h (m)	area A_h (m^2)	num. of rows	num. of houses	total area of houses A_{hsum} (m^2)	Distance between houses (m) ↓	→	width w_g (m)	length l_g (m)	area A_g (m^2)	A_{hsum}/A_g (m^2/ha)	S_g (houses/ha)
A	10,4	13,8	144	3	6	861	13,8	10,4	44	83	3643	2364	16
C	10,4	13,8	144	3	6	861	27,6	10,4	44	124	5465	1576	11
D	10,4	13,8	144	3	6	861	41,4	10,4	44	166	7286	1182	8
G	10,4	13,8	144	2	4	574	13,8	10,4	44	55	2429	2364	16
H	10,4	13,8	144	2	4	574	27,6	10,4	44	83	3643	1576	11
I	10,4	13,8	144	2	4	574	52,2	10,4	44	110	4858	1182	8
E	10,4	13,8	144	3	6	861	13,8	10,4	44	93	4086	2108	15
F	10,4	13,8	144	3	6	861	27,6	10,4	44	134	5907	1458	10

SCALED	**scaling factor**		**50**										
	house			**house group**									
Scale model house group	width w_h (m)	length l_h (m)	area A_h (m^2)	num. of rows	num. of houses	total area of houses A_{hsum} (m^2)	Distance between houses (m) ↓	→	width w_g (m)	length l_g (m)	area A_g (m^2)	A_{hsum}/A_g (m^2/ha)	S_g (houses/ha)
A	13	17,3	224	3	6	1346	17,3	13,0	55	104	5693	2364	11
C	13	17,3	224	3	6	1346	34,5	13,0	55	155	8539	1576	7
D	13	17,3	224	3	6	1346	51,8	13,0	55	207	11385	1182	5
G	13	17,3	224	2	4	897	17,3	13,0	55	69	3795	2364	11
H	13	17,3	224	2	4	897	34,5	13,0	55	104	5693	1576	7
I	13	17,3	224	2	4	897	65,3	13,0	55	138	7590	1182	5
E	13	17,3	224	3	6	1346	17,3	13,0	55	116	6384	2108	9
F	13	17,3	224	3	6	1346	34,5	13,0	55	168	9230	1458	7

Table 10 Parameters characterising the flow.

SCALE MODEL EXPERIMENTS												
	flow depth d (m)				average flow velocity v (m/s)				vd (m^2/s)			
	before		after		before		after		before		after	
Scale model	house models		house models		house models		house models		house models		house models	
house group	min	max	min	max	min	max	min	max	min	max	min	max
A	0,04	0,12	0,03	0,08	0,12	0,27	0,14	0,44	0,0044	0,0329	0,0044	0,0329
C	0,04	0,13	0,03	0,08	0,11	0,25	0,15	0,42	0,0044	0,0328	0,0044	0,0328
D	0,04	0,14	0,03	0,08	0,11	0,24	0,14	0,43	0,0043	0,0333	0,0043	0,0333
G	0,03	0,10	0,03	0,07	0,12	0,25	0,14	0,37	0,0042	0,0249	0,0042	0,0249
H	0,04	0,13	0,03	0,08	0,12	0,27	0,14	0,43	0,0043	0,0332	0,0043	0,0332
I	0,04	0,10	0,03	0,07	0,12	0,23	0,15	0,37	0,0044	0,0238	0,0044	0,0238
E	0,05	0,15	0,03	0,06	0,09	0,16	0,16	0,41	0,0043	0,0250	0,0043	0,0250
F	0,05	0,16	0,03	0,06	0,08	0,16	0,15	0,40	0,0042	0,0250	0,0042	0,0250
all groups	0,03	0,16	0,03	0,08	0,08	0,27	0,14	0,44	0,0042	0,0333	0,0042	0,0333
SCALED												
	min	max	min	max	min		max		min			max
all groups 30x	1,0	4,7	0,8	2,4	0,5	1,5	0,8	2,4	0,7	5,5	0,7	5,5
all groups 40x	1,4	6,3	1,1	3,1	0,5	1,7	0,9	2,8	1,1	8,4	1,1	8,4
all groups 50x	1,7	7,8	1,4	3,9	0,6	1,9	1,0	3,1	1,5	11,8	1,5	11,8

The relation between the Manning's roughness coefficient and flow parameter *vd* is illustrated in Figure 31 and Figure 32. Unlike in the case of forest the different scales (30, 40 and 50) are now presented separately. The experiments A, C, D, G, H and I in which houses were situated lengthways in the flume are presented in Figure 31. These experiments are divided into three categories based on the building coverage parameter A_{hsum} /A_g which was 1182 m^2/ha, 1576 m^2/ha or 2364 m^2/ha. The diagonally placed houses, experiments E and F, are presented in Figure 32. These experiments are divided into two categories based on the building coverage parameter A_{hsum} /A_g: either 1458 m^2/ha or 2108 m^2/ha. The scaled average flow velocity is presented in Figure 33 and Figure 34. The larger values of flow depth were achieved by increasing the discharge, which automatically caused larger values of flow velocity. A certain flow depth could be tested only with a particular discharge. Figure 31 and Figure 32 can be used to estimate the Manning's roughness of a dense built area. Note that the Manning's *n* in Figure 31 and Figure 32 describe the roughness of the buildings and the bottom roughness is not included. In addition the values of *n* were calculated using the whole cross-sectional area of the flume.

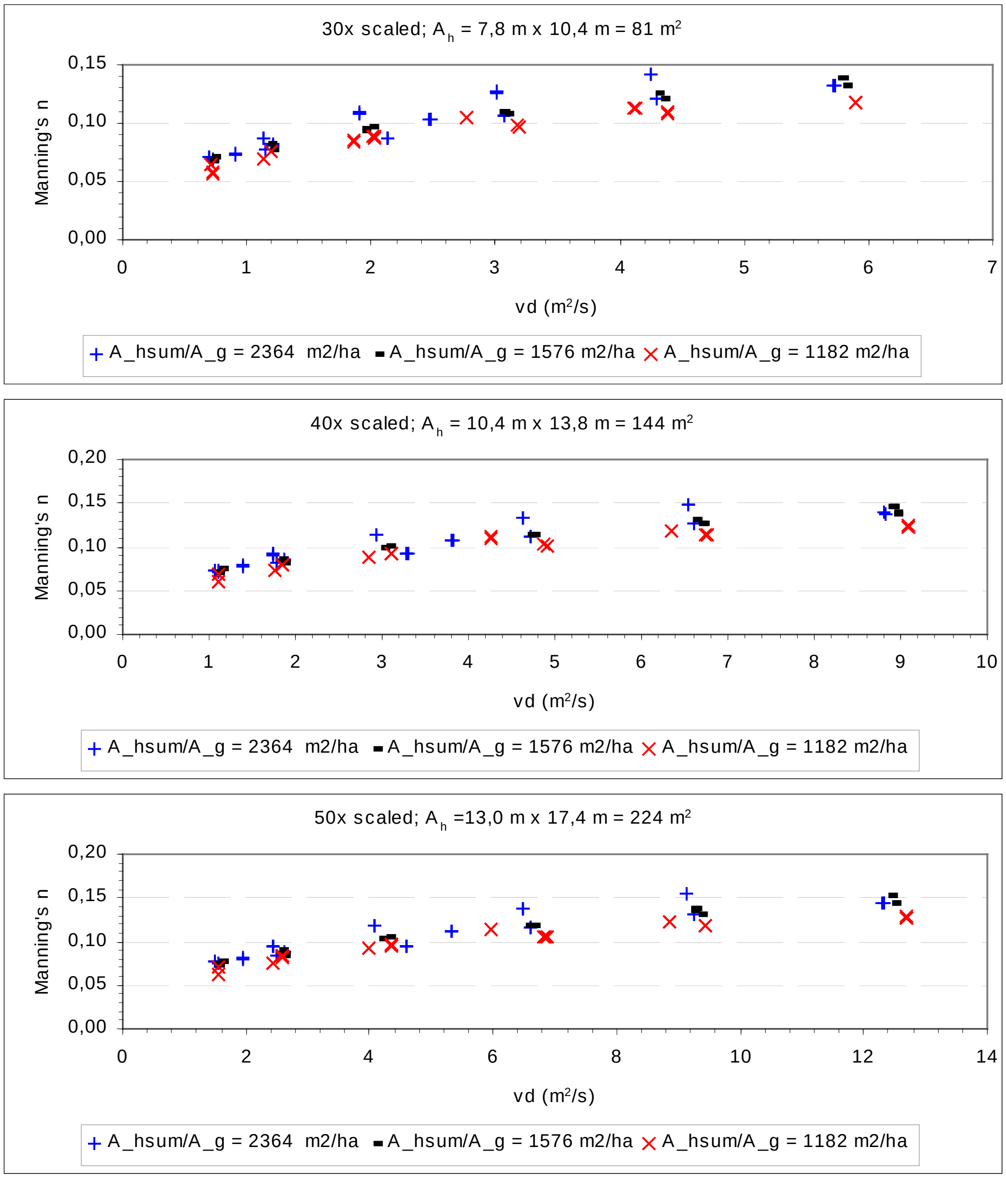

Figure 31 Manning's *n* of house groups A, C, D, G, H & I.

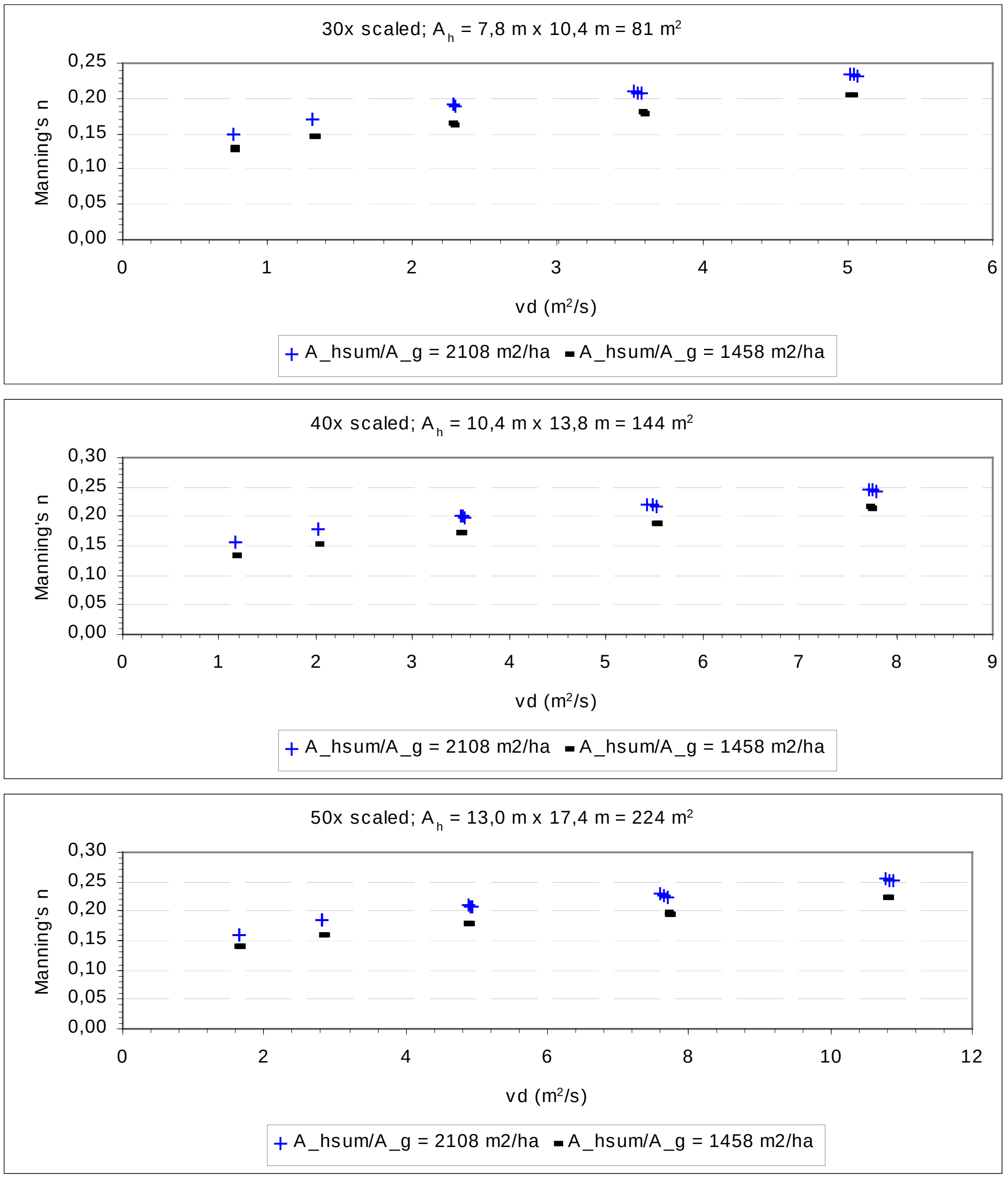

Figure 32 Manning's *n* of house groups E & F.

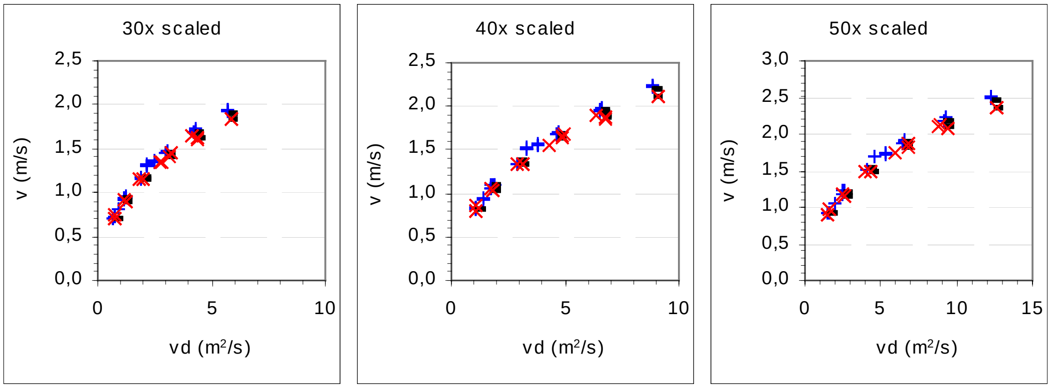

Figure 33 Average flow velocity of house groups A, C, D, G, H & I.

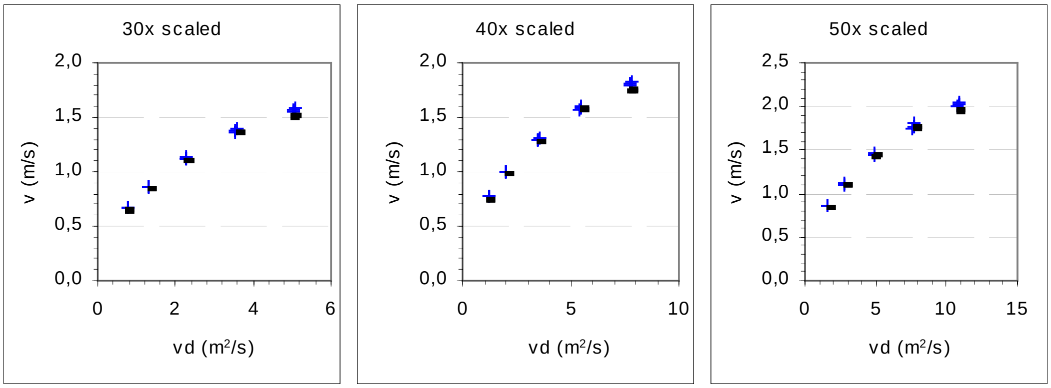

Figure 34 Average flow velocity of house groups E & F.

Other way to deal with the urban area is to reduce the cross-sectional area in the flow direction as shown in Figure 35. It describes the scale model house experiments A, C, D, G, H and I conducted in the fixed bed flume. The width of the flume was 1,1 m, water depth was *d* and cross-sectional area 1,1*d* m^2. There were two adjacent 0,26 m wide house models in the flume. When the cross-sectional area of houses 0,52*d* m^2 is eliminated the reduced cross-sectional area is 0,58*d* m^2 and the reduced width b_r = 0,58 m. In order to carry the same amount of water the roughness in the case of the reduced cross-sectional area n_r must be smaller than the 'normal' *n*. Assuming the same water depth *d* and discharge *Q* as in the experiments the values of n_r were calculated. The calculated and scaled values of n_r are shown in Figure 36 and 37. The values of *n* calculated by using the whole cross-sectional area of the flume and the Manning's roughness n_e of the empty flume are also presented in the Figure 36 and 37. Note that the values of *n* in the case of the whole cross-sectional area are already presented in Figure 31 and 32. The values of n_r are clearly smaller than the values of *n* calculated using the whole cross-sectional area and slightly larger than the values of n_e in the empty flume.

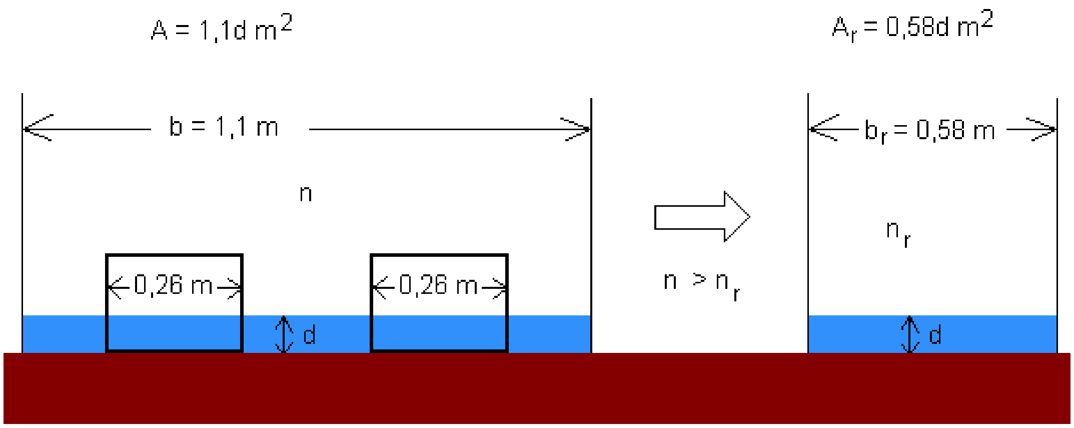

Figure 35 Eliminating the area of houses from the cross-sectional area in flow direction.

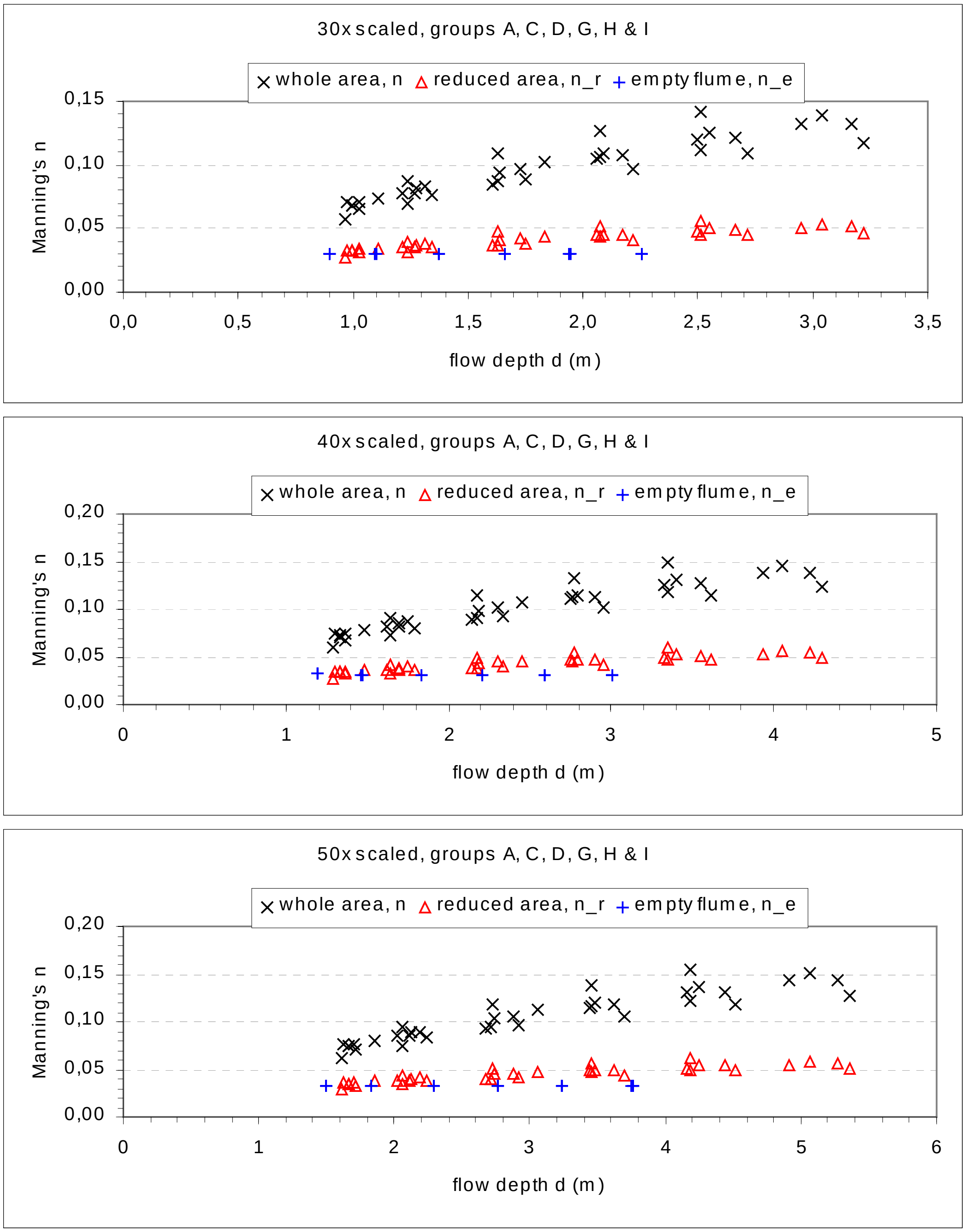

Figure 36 Manning's roughness coefficients n and n_r of house groups A, C, D, G, H & I and the roughness of empty flume.

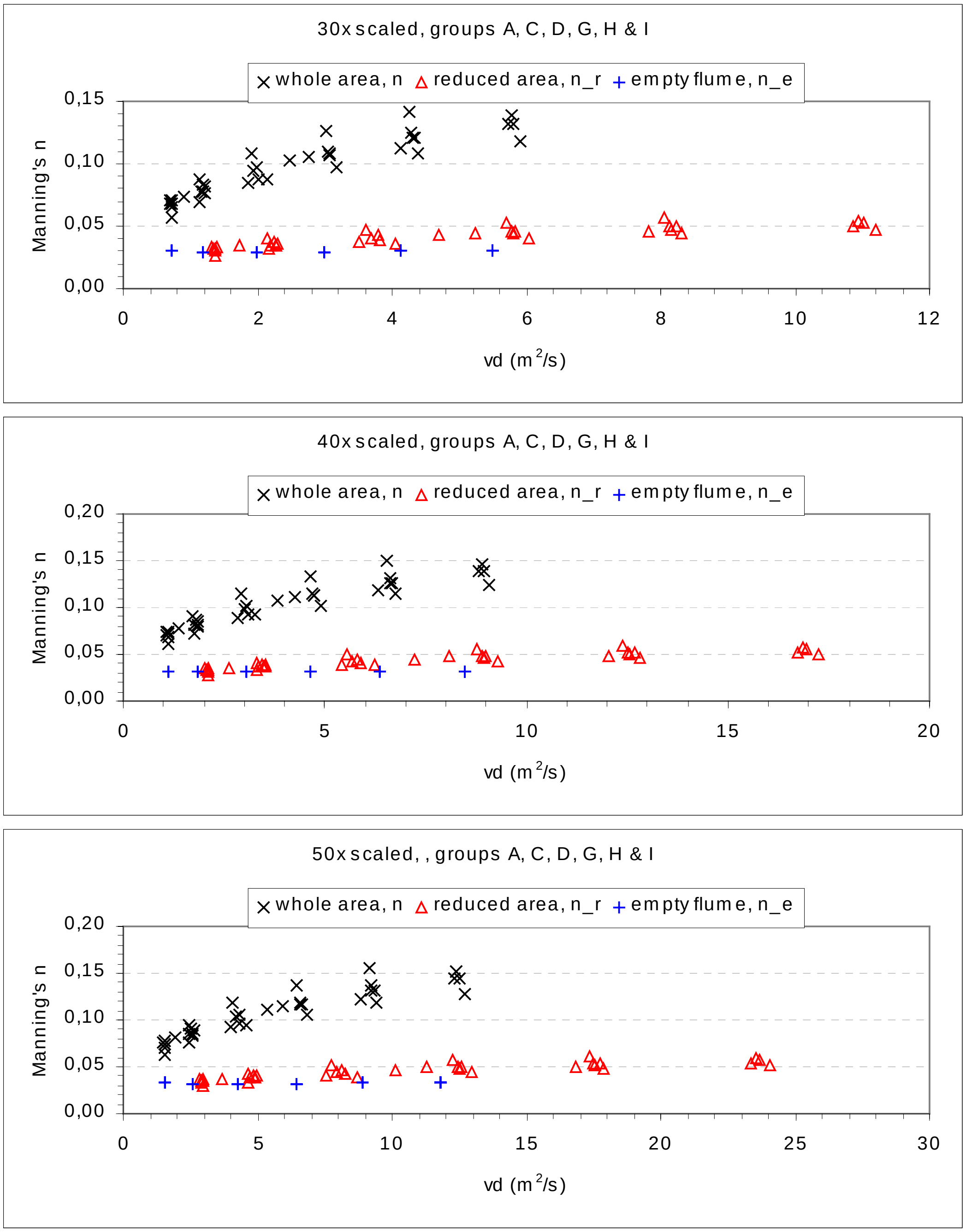

Figure 37 Manning's roughness coefficients n and n_r of house groups A, C, D, G, H & I and the roughness of empty flume.

Using the n_r we can now calculate the 'normal' n backwards, these calculated values are denoted as n_c. First, we calculate the head loss h_f using roughness coefficient n_r, the reduced width b_r and assuming same water depth d and discharge Q as during the experiments. The 'normal' n can now be calculated using the calculated head loss and the flume width b. Values of n_c and the values of n calculated directly using the results of the scale model experiments are presented in Figure 38. We can see that backwards calculated values of n_c are smaller than values of the 'normal' n. This is because the effect of the sequential rows of houses is not taken into account when calculating backwards. Furthermore, we can produce the calculated values of n_c for different cross-sections by calculating the head loss using different reduced widths.

Figure 39 presents the calculated values of n_c for different cross sectional-areas. In Figure 39 the legend indicates the percentage of the flow width which is not occupied by the houses. It is clear that when the percentage of houses in the cross-section increases the roughness coefficient n_c increases. As mentioned earlier, this method underestimates the roughness because the effect of the sequential rows of houses is not taken into account.

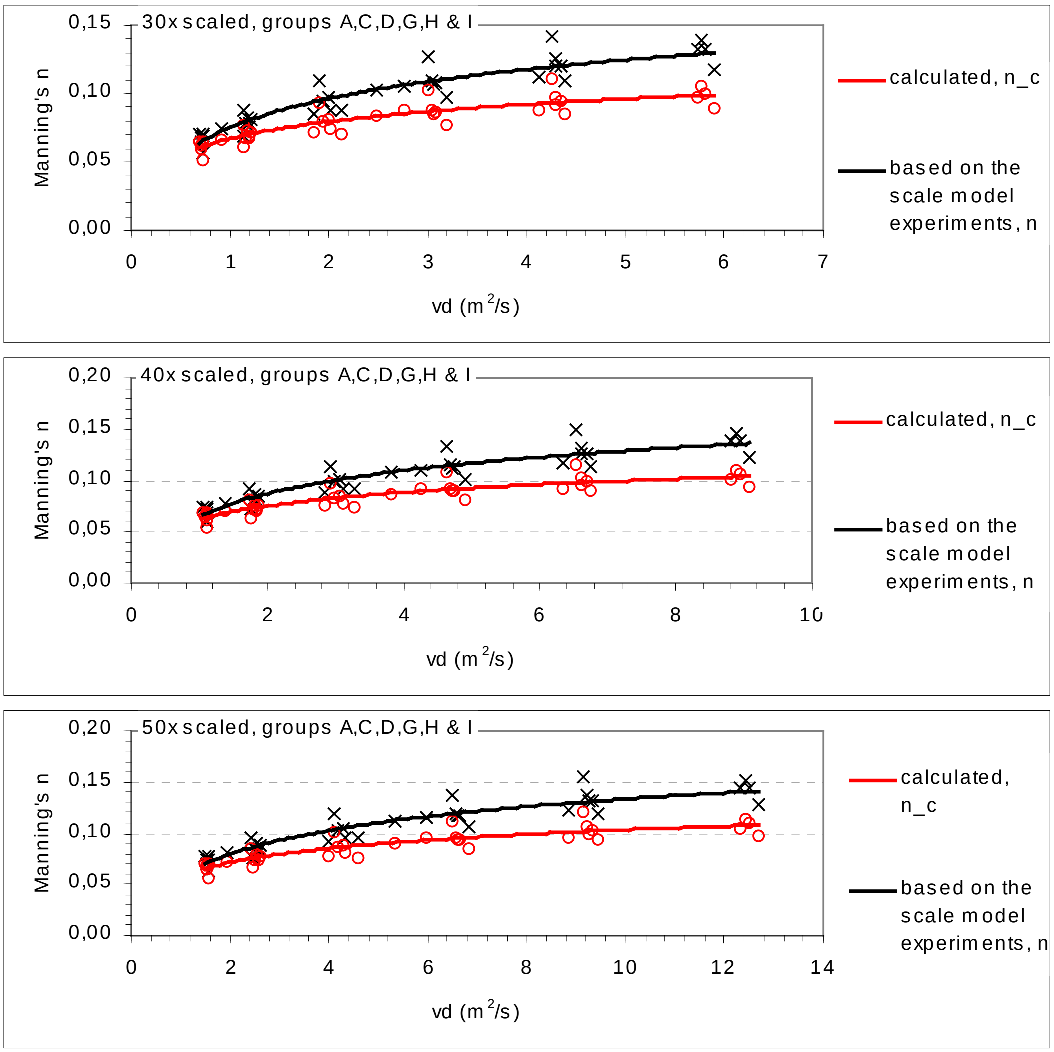

Figure 38 Manning's roughness coefficient backwards calculated n_c and directly calculated n.

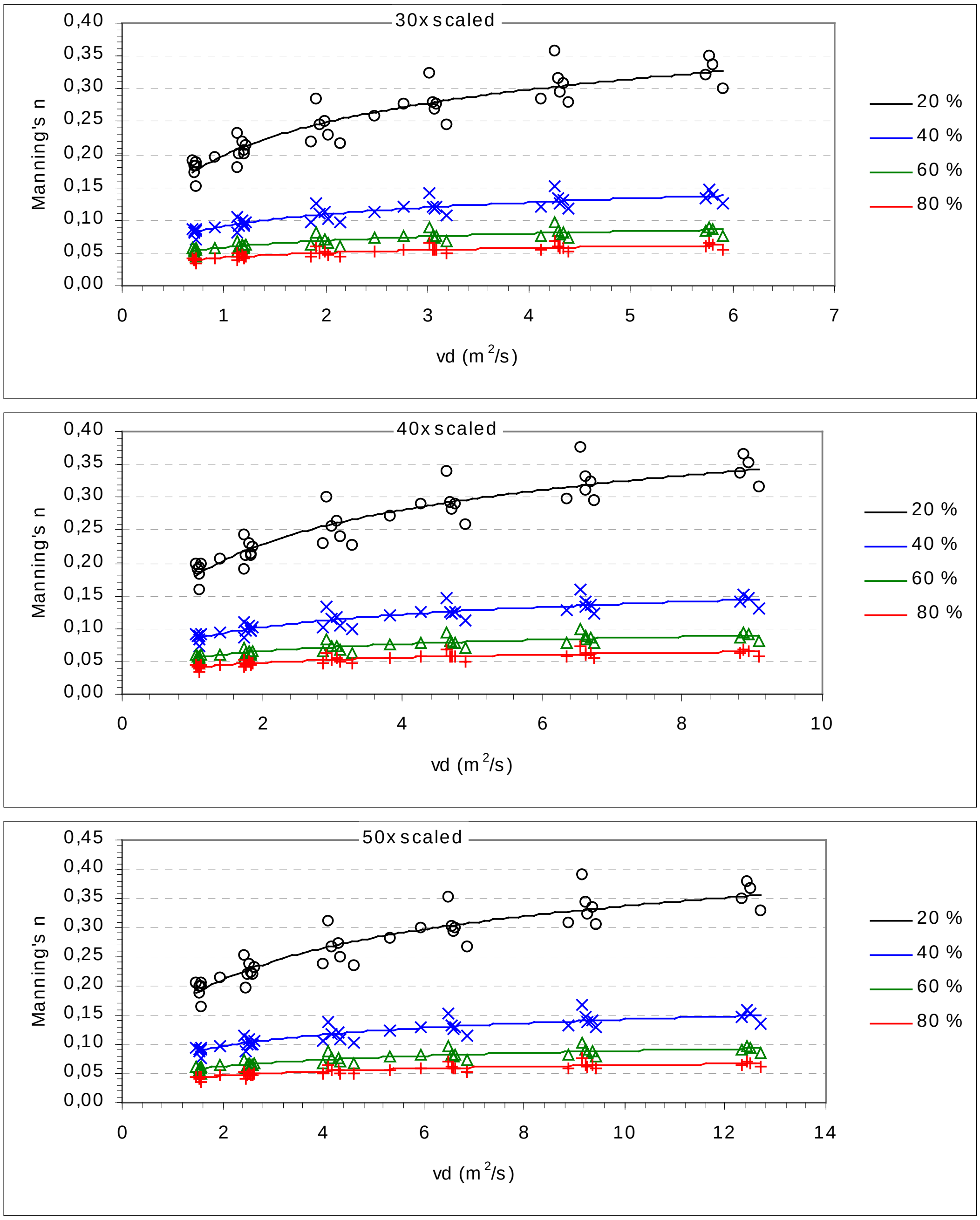

Figure 39 Backwards calculated Manning's roughness n_c.

4. HUMAN STABILITY IN FLOWING WATER

4.1 INTRODUCTION

Flood can be dangerous for an individual due to the depth and velocities of water. Drowning is the number one cause of flood deaths (Federal Emergency Management Agency 1979). It is important to define how human subject can cope with different flow conditions. The knowledge of human limits in the flow helps to determine the time interval, in which the rescue action must be completed.

According to the Federal Emergency Management Agency (1979), a moderate sized person begins to lose stability in 0,91 m (3 ft) deep water flowing 0,61 m/s (2 ft/s). In this case the parameter velocity times depth *vd* is 0,56 m^2/s (6 ft^2/s). A child loses stability in water of lower depths and velocities. Swiftly flowing water which depth is only 15 cm (6 in) can knock you down (Federal Emergency Management Agency 1997). Roberts and Alexander (1982) state as a general rule that water depths greater than 1 m cannot be negotiated by those who cannot swim. It is important to notice that not only residents of the flooded area but also rescue officials are in danger.

4.2 HUMAN STABILITY TEST AT THE COLORADO STATE UNIVERSITY (ABT ET AL. 1989)

4.2.1 Introduction

The first study on human stability in a high flood hazard zone was completed at the Colorado State University in the late 1980´s. The purpose of the study was to find out when the velocity and/or depth of flood flow pose a life threatening hazard. In other words, to identify when an adult human could not stand or manoeuvre in flowing water.

In the study, twenty human subjects (2 female and 18 male) and a rigid body monolith were tested in a recirculating flume. The monolith was assumed to represent the lower limit of human instability. The mass *m* of the human subjects was 41–91 kg (90–201 pounds) and the height *h* 1,52–1,91 m (60–72 inches). The mass of the monolith was 53,4 kg and height 1,52 m. 71 tests were conducted, with 65 tests of healthy human subjects and 6 with monolith. Two flume slopes (1,5 % and 0,5 %) and four different test surfaces, including turf, smooth concrete, steel and gravel were used. Human subjects wore similar clothing (jeans, slacks, pull-over shirts, tennis shoes, thongs, light boots) in order to establish a consistent database.

The *product number (PN)* was used to describe the human survivability in flood flow, thus

$$PN = d \cdot v$$

Equation 8

where *d* is the depth of flow (m) and *v* is the average velocity (m/s).

Theoretical product numbers for the monolith ranged from approximately 0,14 m^2/s to 0,56 m^2/s. These product numbers were from toppling hazard envelope, which was result for solving equation

$$M_{edge} = \{(W\text{-}B) \cdot (0{,}5 \cdot thickness)\} - \{P \cdot 0{,}5d\} = 0$$

Equation 9

where ΣM_{edge} is the sum of moments about the downstream edge of the monolith, W is the weight of monolith (N), B is the buoyancy (N), *thickness* (m) refers to the monolith and P is the dynamic force due to velocity (N). Equation 9 was the result for summing moments about the downstream bottom edge of the monolith.

4.2.2 The summary of test results and the experimental bias

When the experiment started, the product number was pre-set to 0,56 m^2/s for all test persons. During the test time different combinations of the water depth and velocity were used until the test subject lost stability in the flow. The analysis of experimental data was performed using Equation 8. As a result, the product numbers for human subjects varied between 0,70 m^2/s and 1,94 m^2/s for channel slope 1,5%. The product numbers for channel slope 0,5% were between 0,93 m^2/s and 2,13 m^2/s. These values were naturally larger than the corresponding values for the monolith, because the human subject possess the innate skill to compensate for varying flow conditions and bed slope by adjusting the body stance and body position. Generally, the product numbers in the test were larger for taller and heavier persons than for smaller and lighter persons. The product numbers for monolith ranged for both channel slopes from 0,22 m^2/s to 0,39 m^2/s. The test results are presented in Figure 40.

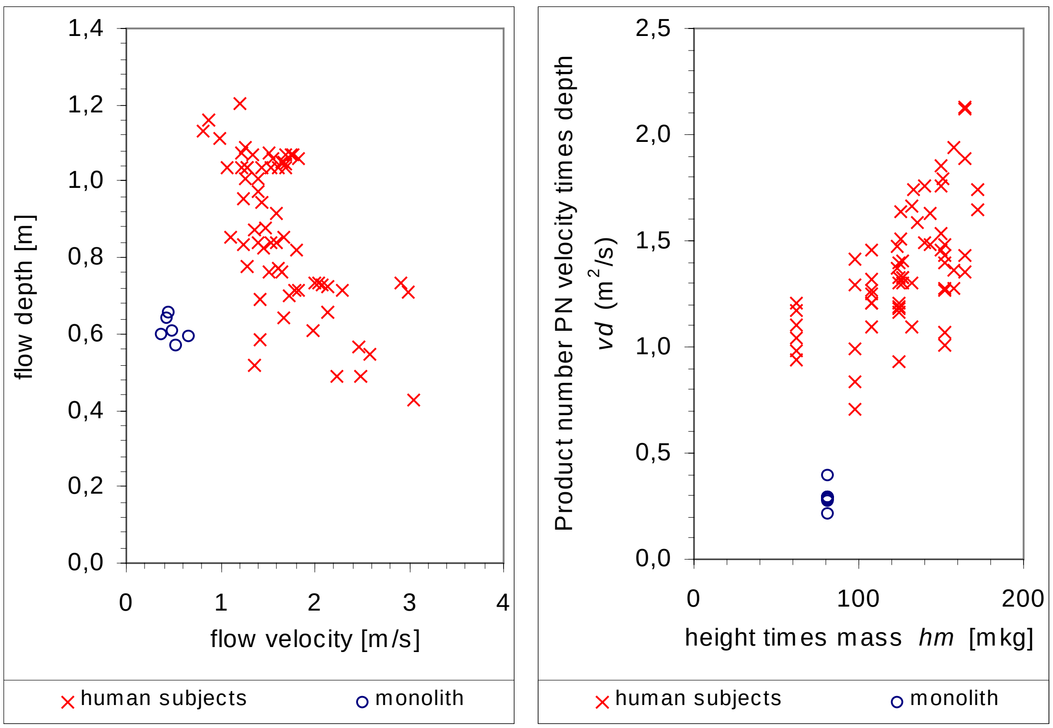

Figure 40 Flow conditions which caused loss of stability or manoeuvrability (Based on Abt et al. 1989).

Because of the experimental procedures and constraints, the results did not fully reflect the real flood flow situation. According to Abt et al. (1989), the study bias and constraints included:

– the test persons were influenced by the presence of safety equipment

– the test persons learned to manoeuvre in the flow with time

– two hour testing session included 2-4 tests, which might in some cases fatigued a test person

– the test conditions were optimal, in other words lighting conditions were good and there was no debris flow in the water. Water temperature varied between 20 ºC and 26 ºC.

– the test persons age ranged from 19 to 54 year and they all were in good health
– the test persons did not carry any additional loads.

4.3 HUMAN STABILITY TEST OF THE RESCDAM PROJECT

4.3.1 Introduction

One part of the RESCDAM experiment program were tests with the human subjects in order to define the limits for a safe rescue action in the case of a dam-break flood. Practically, this meant the combination of flow depth and velocity into the product number $PN = d \cdot v$, which describes the human survivability in the flood flow as mentioned in chapter 4.2.

4.3.2 Experimental apparatus

The experiments were conducted at the model basin of Helsinki University of Technology Ship Laboratory. The model basin was 130 m long and 11 m wide with a depth of approximately 5,5 m and the water temperature was about 16 °C. The model basin was equipped with a towing carriage which maximum speed was 8 m/s.

Figure 41 Model basin and the towing carriage.

Human subjects were tested on a special platform structure (Figure 42) which was specially designed and constructed. The structure had a steel beam (50 mm × 50 mm & 50 mm × 100 mm) framework and a steel grating. The grating was made of two parts (48 cm × 117 cm and 63 cm × 150 cm) located side by side. The width of the grating was 113 cm and the length 117 m / 150 m. The platform structure was installed on the towing carriage and served as a rack for the human subjects. The structure was vertically adjustable and depths from 10 cm to 110 cm were attained.

Figure 42 The platform structure (left) fastened to the towing carriage (right).

4.3.3 Human subjects

Seven human subjects were tested: five males and two females; height 1,60–1,95 m; mass 48–100 kg; age 17–60 years (Table 11). The human subjects 1 and 2 were professional rescuers. All human subjects tested were wearing Gore-Tex survival suits (Figure 43) and subject 3 was tested also with waders (Figure 44). All human subjects wore safety helmet and were tethered with a safety rope. In addition, there was a handle and a second safety rope which could be used when a subject lost stability.

Table 11 Human subjects.

	sex	**age** (years)	**height** (m)	**mass** (kg)	**height x mass** (m x kg)
1	male	28	1,70	69	117
2	male	31	1,95	100	195
3	male	28	1,79	76	136
4	female	32	1,62	57	92
5	male	60	1,82	94	171
6	female	17	1,60	48	77
7	male	19	1,74	71	124

Figure 43 Human subject 4 wearing Gore-Tex survival suit, safety belt and safety helmet.

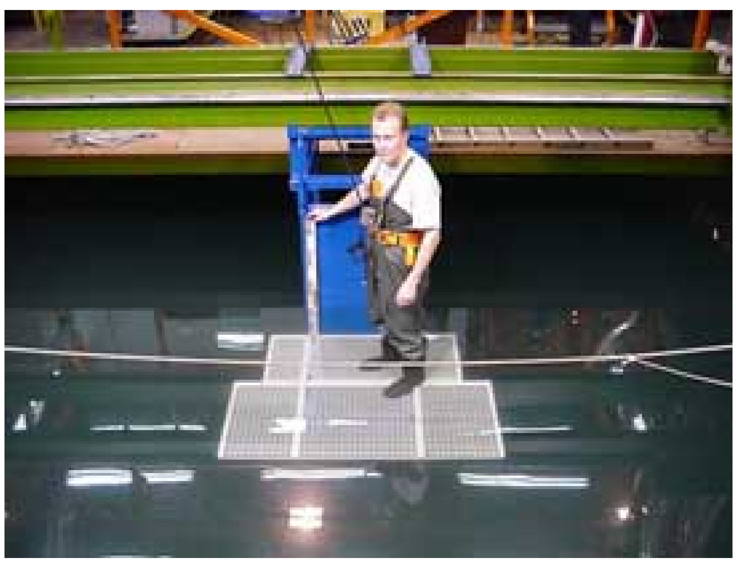

Figure 44 Human subject 3 wearing waders and safety belt. Subject tethered with safety rope.

4.3.4 Experimental procedure

Each human subject was individually tested in several water depths. Before the experiment each subject was allowed to become familiar with the test facility and safety equipment in stagnant water. The initial water depth was set and the initial velocity was then chosen. The initial conditions were chosen so that the product number *vd* was low enough and it was easy to wade. A human subject was asked to walk into the flow, walk perpendicular to the flow and face downstream to the flow. If a subject maintained manoeuvrability, the velocity was gradually increased. This was continued until the subject lost stability or manoeuvrability

(Figure 45 and Figure 46). Once the stability was lost, the towing carriage was immediately stopped. The water depth and velocity were recorded and the human subject was shortly interviewed. The experiment was continued with the next depth and proceeded until at least four depths were tested. The experimental procedure was carried out with all seven human subjects and both photographed and videotaped.

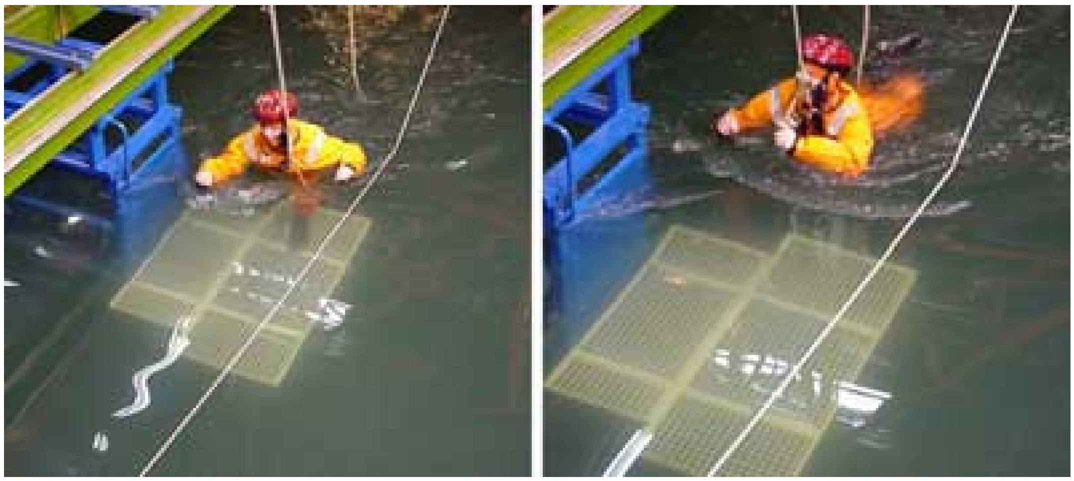

Figure 45 Human subject 1; depth = 1,1 m; velocity = 0,7 m/s.

Figure 46 Human subject 5; depth = 1,07 m; velocity = 1,0 m/s.

4.3.5 Experimental results

Seven human subjects were tested in the experimental program. Velocities 0,6 – 2,75 m/s and water depths 0,3 – 1,1 m were used. Due to the individual properties, there exists a wide range of product numbers *vd* describing a person's manoeuvrability in the flow. The product number *vd* causing loss of stability or manoeuvrability varied from 0,64 m^2/s to 1,26 m^2/s. Taller and heavier individuals managed better in flowing water. (Figure 47 and Figure 48)

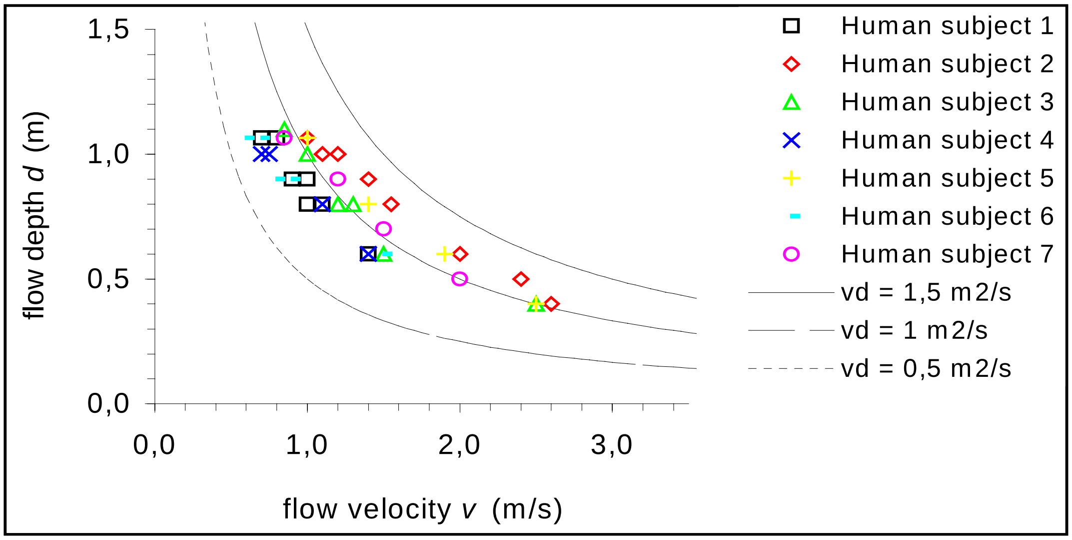

Figure 47 Test results. Loss of stability or manoeuvrability.

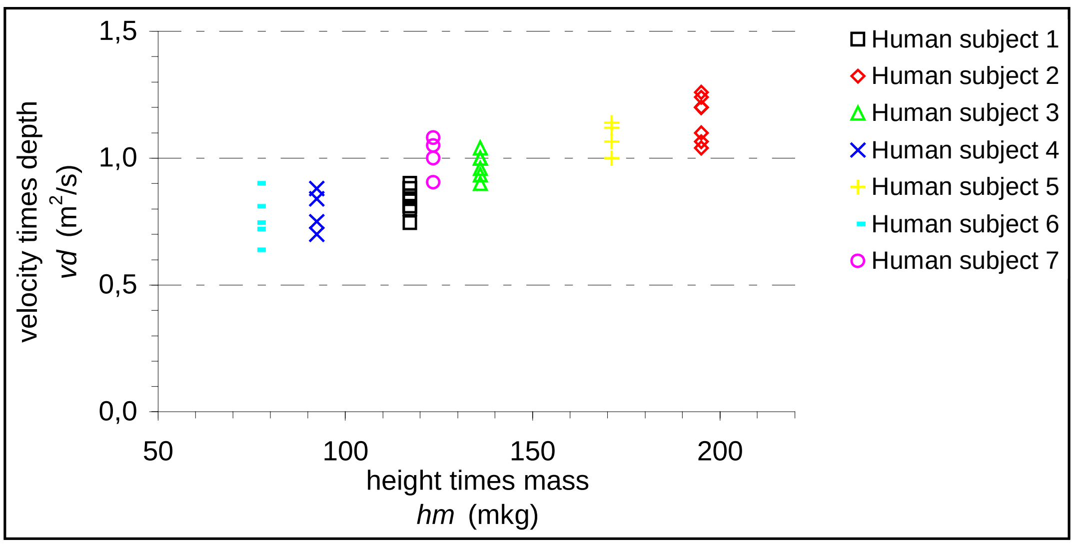

Figure 48 Test results. Loss of stability or manoeuvrability.

4.4 SUMMARY AND CONCLUSIONS

The product numbers *vd* of the RESCDAM project and the study of Colorado study by Abt et al. (1989) are compared in Figure 49. The product numbers of the RESCDAM study are smaller. Some explanations for the difference between the RESCDAM study and Abt et al. may be found.

- Different clothing: In the RESCDAM study a survival suit was used. Some air was trapped inside the suit causing the increase of buoyancy. In addition, the cross-sectional area of a human subject is apparently larger while wearing a survival suit instead of jeans and a T-shirt.

This means that a greater hydrodynamic force affects the subject and makes it more difficult to move against the flow and maintain stability.

- Bottom material: In the RESCDAM study the bottom was quite slippery which made it more difficult to manoeuvre in the flow.

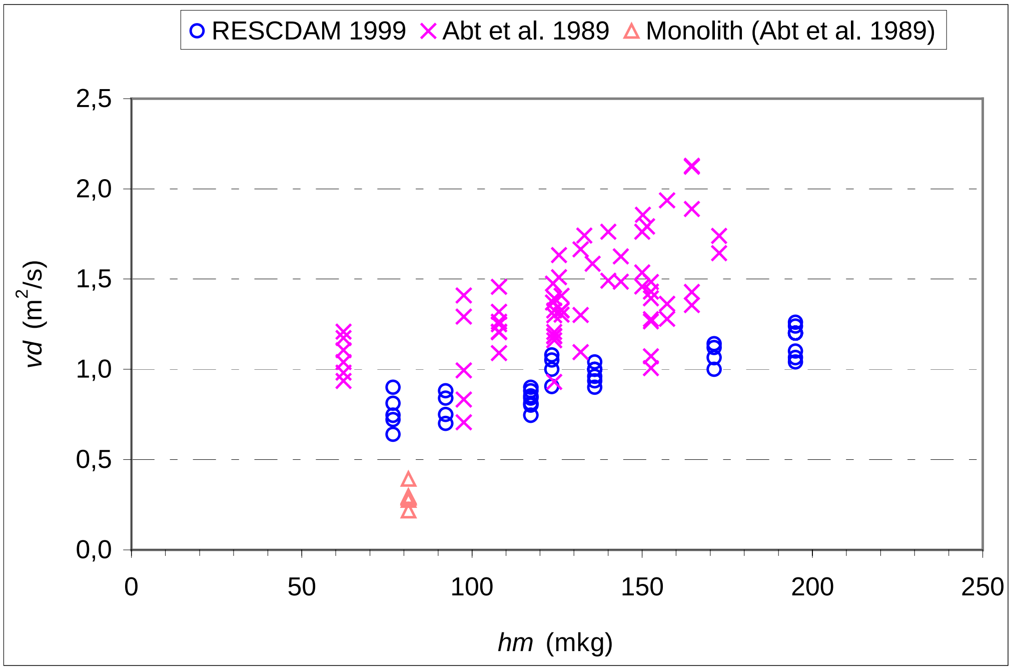

Figure 49 Results of the RESCDAM project and the study of Abt et al. (1989).

The study constraints according to Abt et al. (1989) were optimal test conditions, the presence of the safety equipment and a test subject's ability to learn to manoeuvre in the flow with time (Chapter 4.2.2). The same constraints are surely valid in the RESCDAM study. There is no doubt that the product numbers would be considerably smaller if the forces of nature would be present. For example, during spring floods the weather conditions in Finland can be difficult and there is always some floating debris in the extremely cold water. Floods can also spread into the areas which can be quite unsmooth and rough. Despite of these shortcomings the results of the RESCDAM and Colorado study programme give a conception of the limits of human stability in flowing water.

Based on the studies of Abt et al. (1989) and RESCDAM project, the approximate limits of adult human manoeuvrability and stability in flowing water are given. The limits are valid for adults in flowing water without any special instruments, such as a rope, excluding a survival suit. Children's ability to cope with the flow were not studied, but a child should never attempt to cope with the flow without assistance. The conditions of the flow and environment are divided into three categories: poor, normal and good. The factors affecting the conditions are described in Figure 51. The limits of human manoeuvrability are presented in Figure 50. In good conditions an adult is able to manoeuvre if $vd < 0{,}006hm + 0{,}3$, where v = flow velocity (m/s), d = flow depth (m), h = height of the adult (m) and m = mass of the adult (kg). If the conditions are poor, the limit of manoeuvrability is $vd = 0{,}002hm + 0{,}1$.

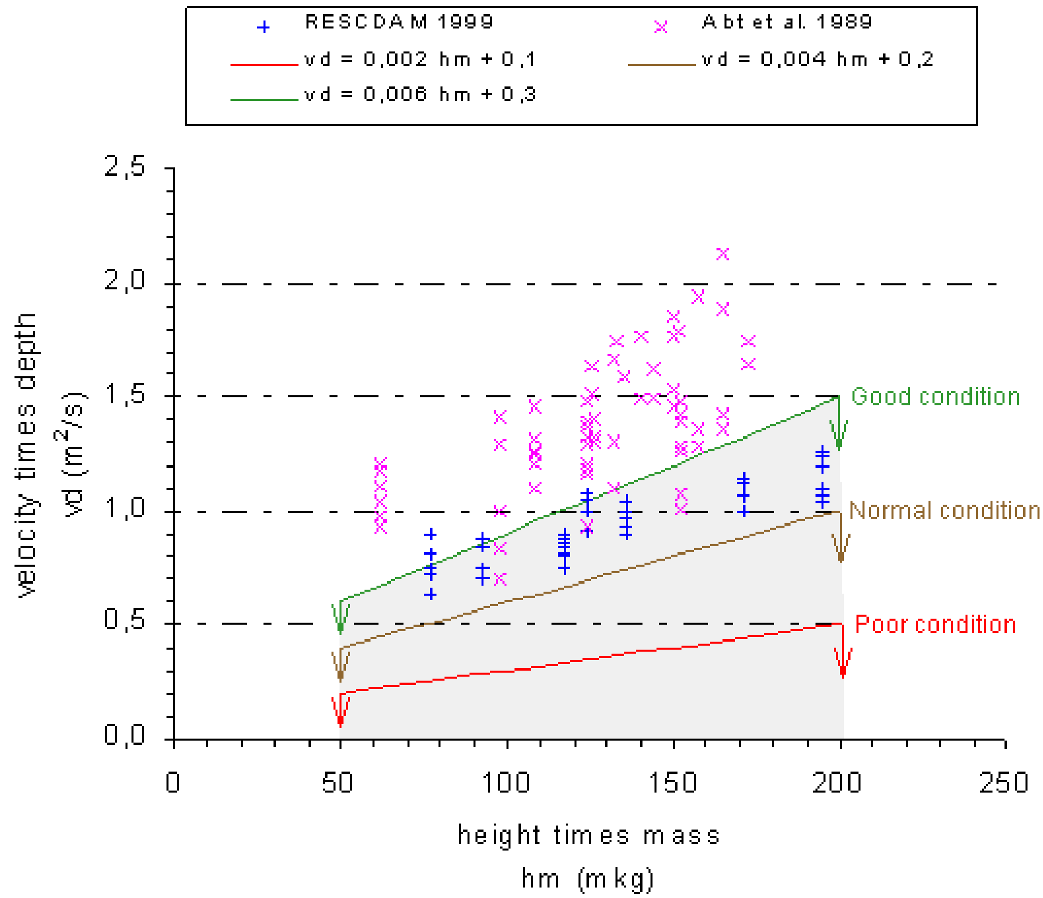

Figure 50 Recommendations for human stability in flowing water.

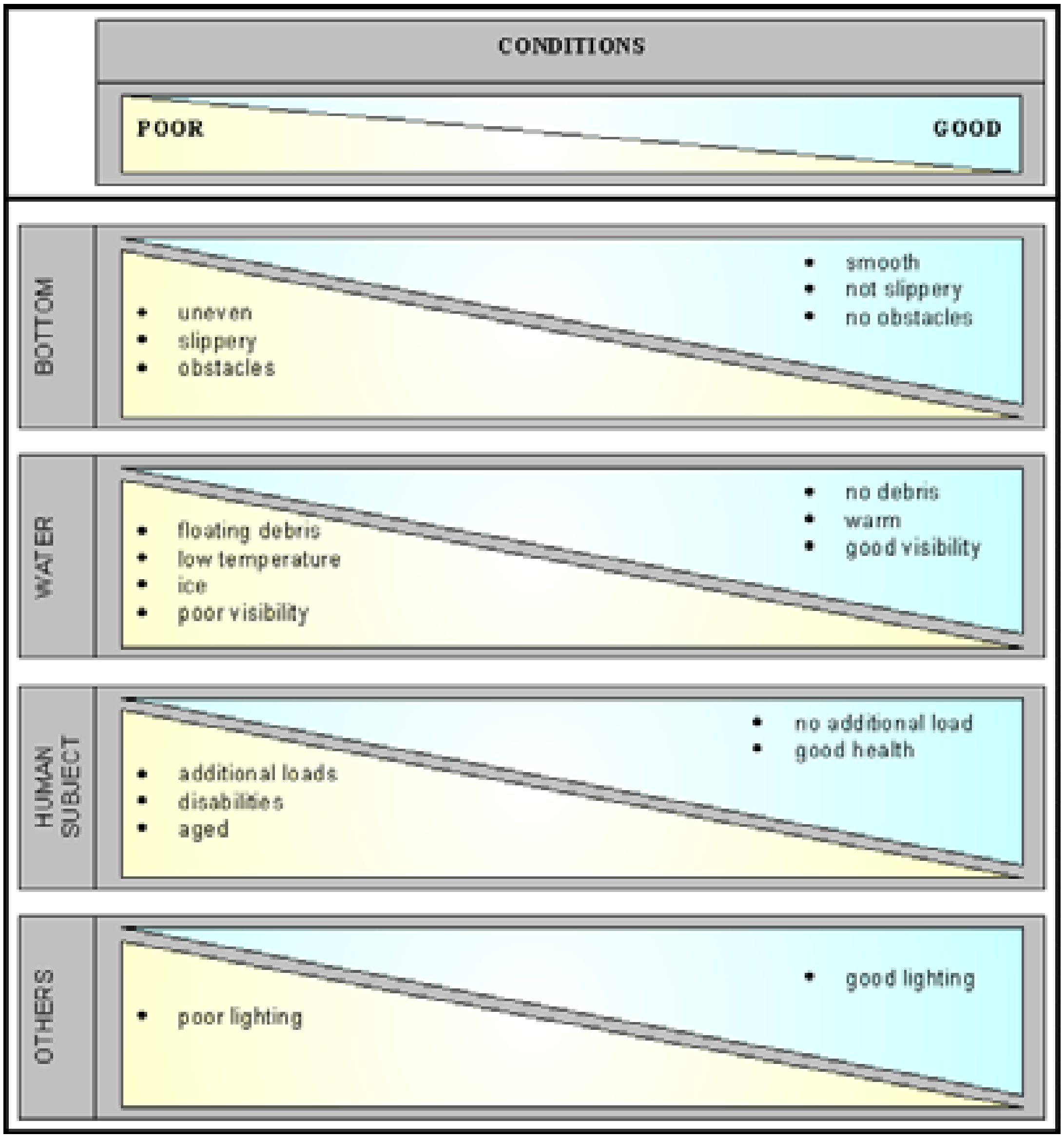

Figure 51 Human subject in flowing water, categories of conditions.

5. SUMMARY

There were three goals in the project: 1) human stability and manoeuvrability in flowing water, 2) permanence of houses in flowing water and 3) roughness coefficients of forest and houses. The manoeuvrability of seven test persons, characterised with the parameter: height times mass *hm* (mkg), was tested in the laboratory using velocities of 0,6 – 2,75 m/s and water depths of 0,3 – 1,1 m. The parameter velocity times depth *vd* (m^2/s) causing the loss of manoeuvrability or stability were attained and the relation between *vd* and *hm* was studied. The results were compared to the earlier study by Abt et al. (1989). Based on the results of these two studies, approximate limits of the adult human manoeuvrability and stability in flowing water were presented (Figure 50 and Figure 51).

The permanence of houses in flowing water was determined by studying literature (Black 1975; Clausen and Clark 1990; Lardieri 1975; Lorenzen et al. 1975; Sangrey et al. 1975; Smith 1989, 1991 & 1994). The findings of the earlier studies were combined and a recommendation for the Finnish houses was made (Table 3).

The scale model experiments were conducted to define the roughness of forests and groups of buildings. The scale model forests and house groups were placed into a fixed bed flume. The difference in water table caused by the scale models was measured in different flow conditions, i.e. different water depths and velocities. The Manning - Strickler – coefficient *n* was used to describe the roughness of the trees in the forest and houses in a built area. The bottom roughness was not included in the test results. The Manning's coefficients were calculated and the results were converted into real scale according to the Froude model law using scale numbers 5, 10 and 20 for the forests and 30, 40 and 50 for the house groups. The house groups were approached by two different ways: 1) The roughness coefficient *n* was calculated using the whole width of the flume and 2) The roughness coefficient n_r was calculated using the width of the flume subtracted by the width of the houses. The relationship among the Manning's roughness coefficient and parameters characterising the flow, the forest and the group of houses was produced. The results for the forest are presented in figures 23, 24 and 25. In the case of the house groups, the roughness *n* is presented in Figure 31 and Figure 32 and the roughness n_r is presented in Figure 36 and Figure 37.

6. REFERENCES

Abt, S.R.; Wittler, R.J.; Taylor, A.; Love, D.J. 1989. Human stability in a high flood hazard zone. Water resources bulletin, American water resources association, August 1989. Vol. 25, No.4, pp. 881-890.

Black, R.D. 1975. Flood Proofing Rural Residences. A Project Agnes Report, Pennsylvania. New York State Coll of Agriculture and Life Sciences, Ithaca. Prepared for Economic Development Administration, Washington, DC Office of Technical Assistance.

Chow, V.T. 1973. Open-channel hydraulics. International edition 1973. Singapore: McGraw-Hill, 1973. 680 pages. ISBN 0-07-085906-X.

Clausen, L. & Clark, P.B. 1990. The development of criteria for predicting dambreak flood damages using modelling of historical dam failures. In: International Conference on River Flood Hydraulics, edited by W. R. White. 17. - 20. September, 1990. John Wiley & Sons Ltd. Hydraulics Research Limited, 1990. pp. 369-380.

Federal Emergency Management Agency. 1979. The floodway: a guide for community permit officials. US Federal Insurance Administration, Community Assistance Series, No.4, 1979.

Federal Emergency Management Agency. 1997. FEMA News Room. FEMA offers flood safety tips. Updated: Updated: January 7, 1997. http://www.fema.gov/DIZ97/fl001.htm

Harrison, S. 1964. A complete history of the great flood at Sheffield on March 11 and 12, 1864.

Kobus, H. 1980. Hydraulic modelling. German association for water resources and land improvement, Bulletin 7, Stuttgart. 339 pages.

Kuuskoski, M. 1948. Mallikokeiden käytöstä vesirakennussuunnittelussa. In: Maanviljelysinsinööriyhdistyksen vuosikirja. Helsinki, 1948. pp. 12-44. *(In Finnish)*

Lardieri, A. C. 1975. Flood proofing regulations for building codes. Journal of the hydraulics division, September 1975. pp. 1156-1169.

Lorenzen, R. T.; Black, R. D.; Nieber, J. L. 1975. Design aspects of buildings for flood plain locations. ASAE Paper, 68th Annu Meet, Davis, Jun 22-25 1975 ASAE St. Joseph, Mich 20p Paper: 75-4037. 19 pages.

Mertens, W. 1994. Zum Strömungswiderstand naturnaher Fließgewässer. Wasserwirtschaft 84 (1994) 3. pp. 138-141.

Novak, P.; Cábelka, J. 1981. Models in hydraulic engineering. Physical principles and design applications. Pitman Advanced Publishing Program. London, 1981. 459 pages. ISBN 0 273 084364.

Roberts, C. P. R.; Alexander, W. J. R. 1982. Lessons learned from the 1981 Laingsburg flood. Civil Engineer in South Africa, Vol. 24, No.1, January, 1982. pp. 17-27.

Sangrey, D.A.; Murphy, P.J. & Nieber, J.L. 1975. Evaluating the impact of structurally interrupted flood plain flows. Cornell University. Prepared for: Office of Water Research and Technology. Distributed by: NTIS. PB-247 552.

Smith, D. I. 1989. A dam disaster waiting to break. New Scientist, 11th November 1989. pp. 42-46.

Smith, D. I. 1991. Extreme floods and dam failure inundation implications for loss assessment. Proceedings of a Seminar "Natural and Technological Hazards: Implications for the Insurance Industry", 1991. pp. 149-165.

Smith, D. I. 1994. Flood damage estimation - A review of urban stage-damage curves and loss functions. Water SA, Vol. 20, No. 3 July 1994. p. 231-238

US Army Corps of Engineers. 1988. "Flood damage analysis package: users manual". USACE, Hydraulic Engineering Centre, Davis, CA.

Water Words Dictionary. 2000. Nevada Division of Water Planning. Department of Conservation and Natural Resources. http://www.state.nv.us/cnr/ndwp/dict-1/waterwds.htm